

SIZE MATTERS

Mechanical Properties of Nano-sized Single Crystals

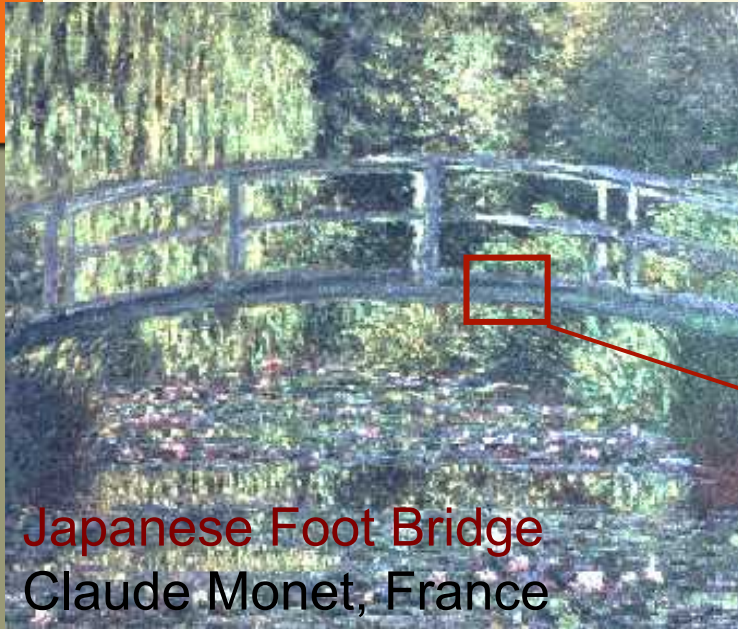
Julia R. Greer

But really it's the work of
graduate student A.T. Jennings
and post-doc Ju-Young Kim

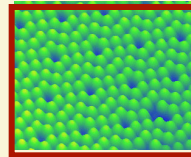
Division of Engineering and Applied Science
California Institute of Technology



Materials and Length Scales



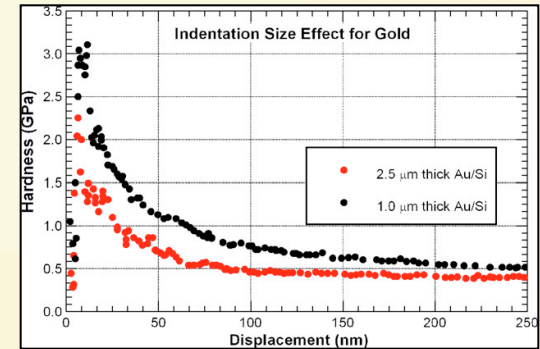
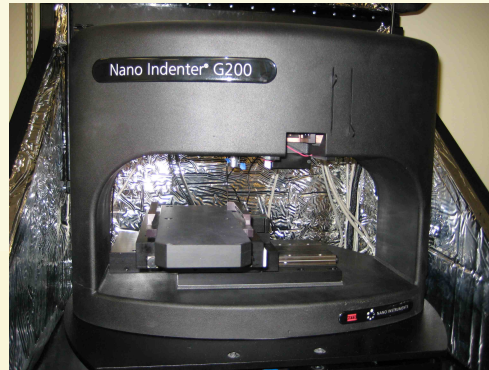
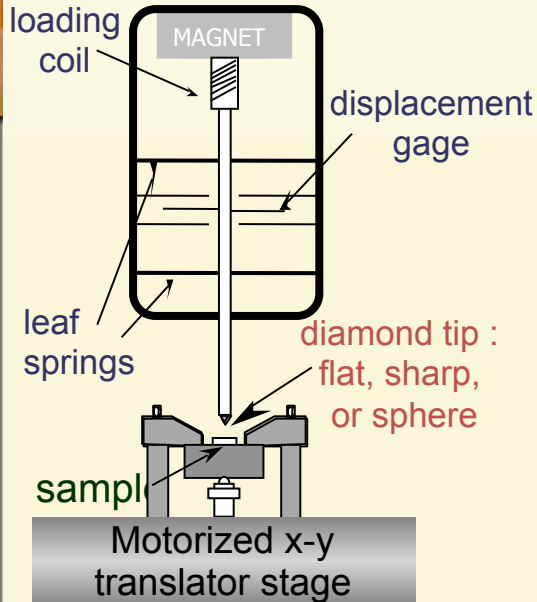
Japanese Foot Bridge
Claude Monet, France



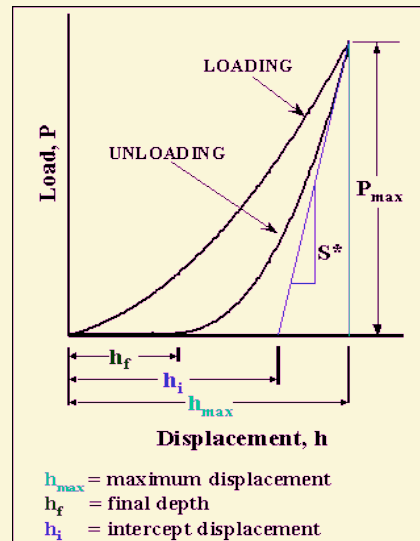
Golden Gate Bridge
San Francisco, CA

In nanocrystals (quantum dots, nanowires, nanotubes, etc.) size modification tunes a variety of properties: optical, electronic, plasmonic, thermal, acoustic, etc. which brings into question **material structural integrity**

Background: Nanoindentation

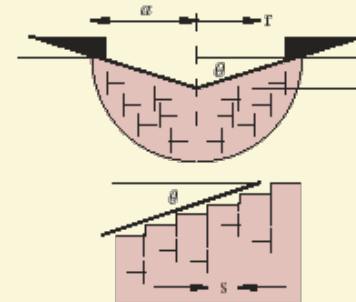


Nix, Feng, Greer, et al Thin Solid Films (2007)



VanLandingham, M.R. et al (2003)

Geometrically Necessary Dislocations



$$\rho_{GND} = \frac{3 \tan^2 \theta}{2bh}$$

$$\therefore \left(\frac{H(h)}{H_0} \right)^2 = 1 + h^* \times \frac{1}{h}$$

strain gradients drive hardness increase!

Disadvantages: Strain gradients, complex stress-strain calculations, limited plasticity information

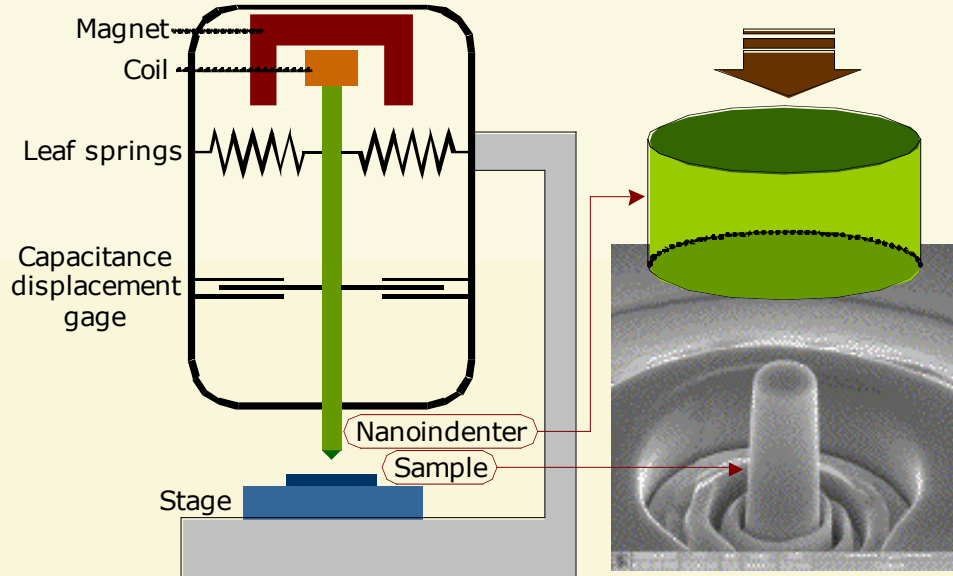
Advantages: Elastic properties, hardness, deformation volume control

Great need for experimental techniques testing mechanical deformation at nano-scale *without* strain gradients!



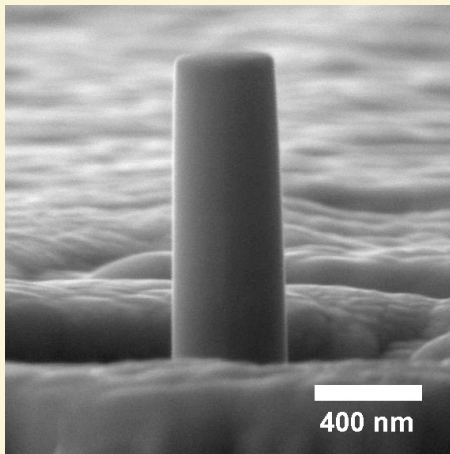
Micro-compression experimental setup

Nanoindenter
Agilent G200



- Flat punch indenter tip
- Constant displacement rate

Nano-pillar fabrication:
Mainly Focused Ion Beam (FIB)



- Diameter: 100 ~ 900 nm

Load-Displacement Data

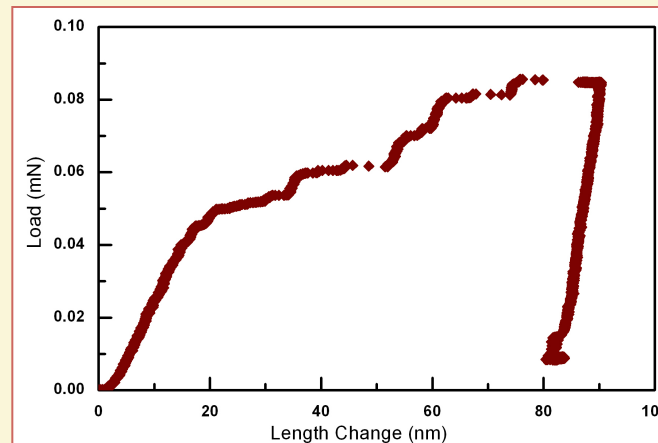
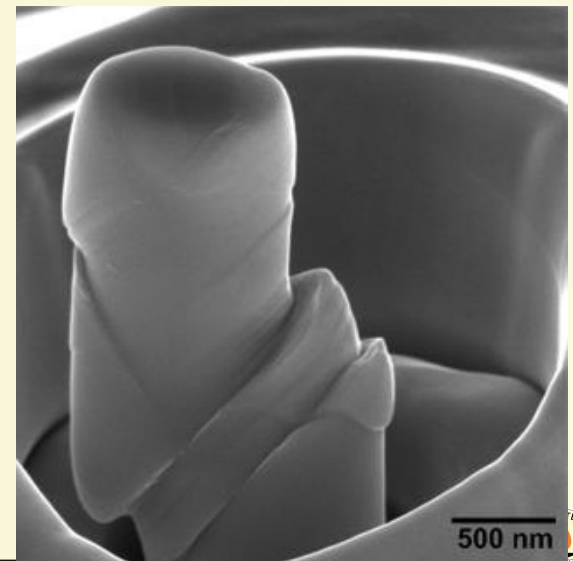
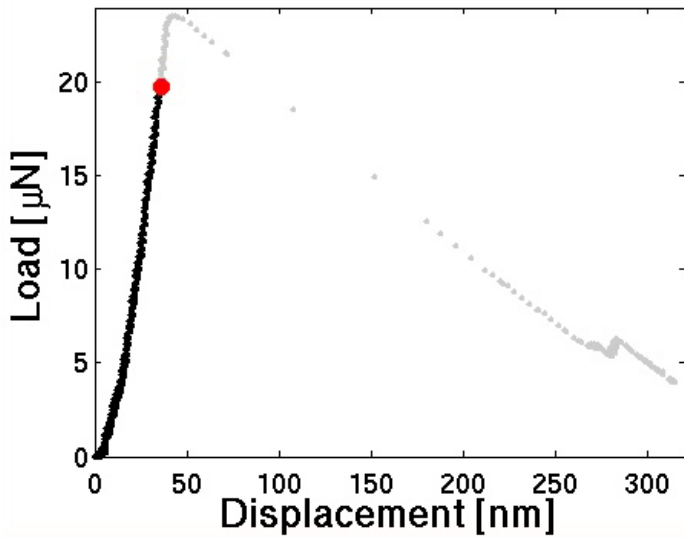
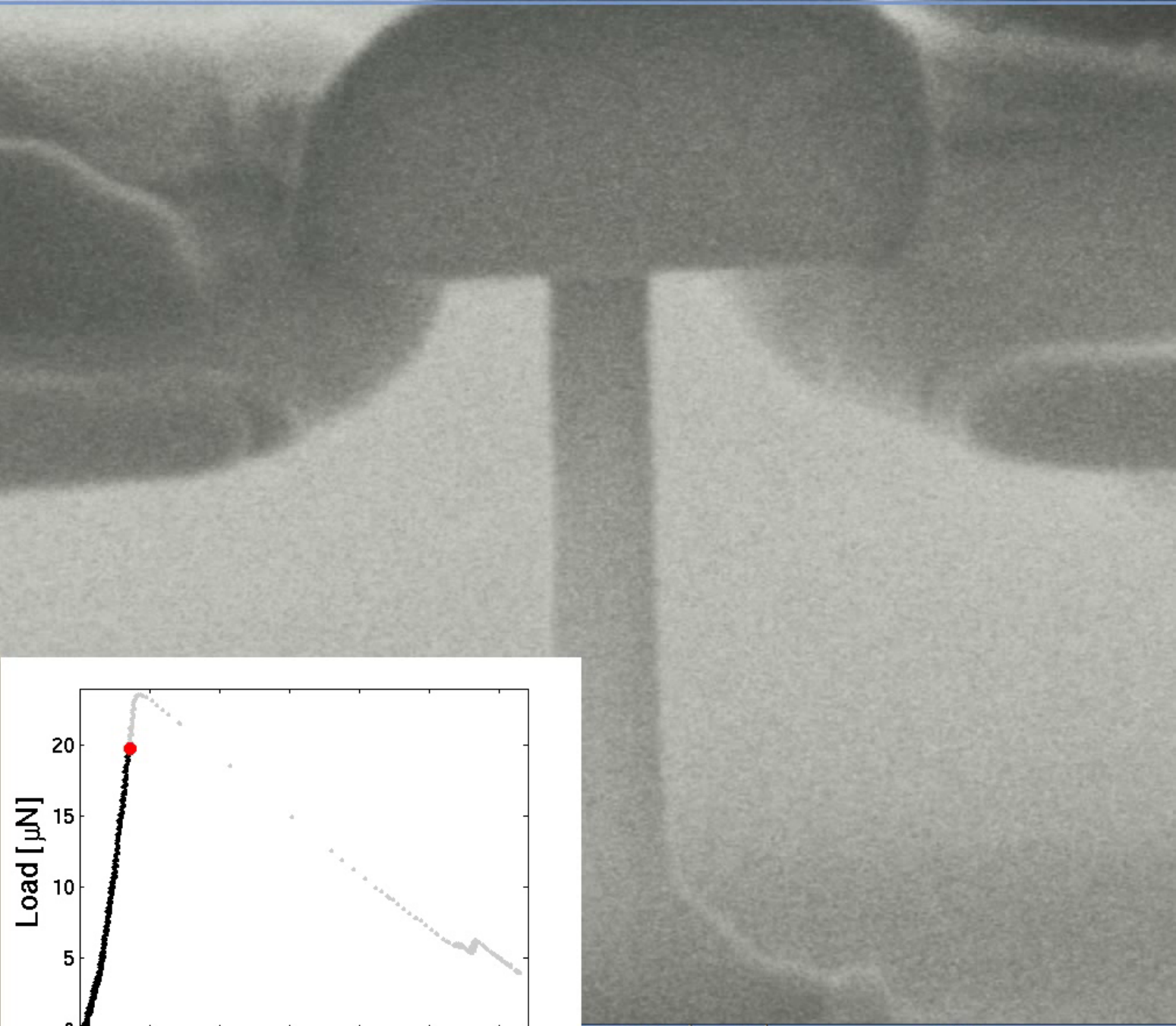
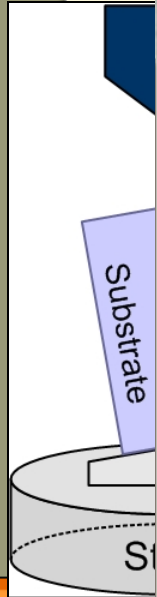
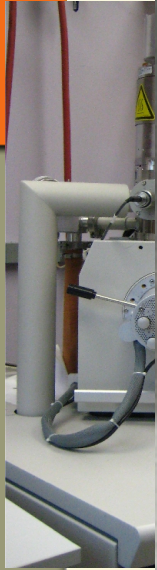


Image after compression





HFW
1.86 μm

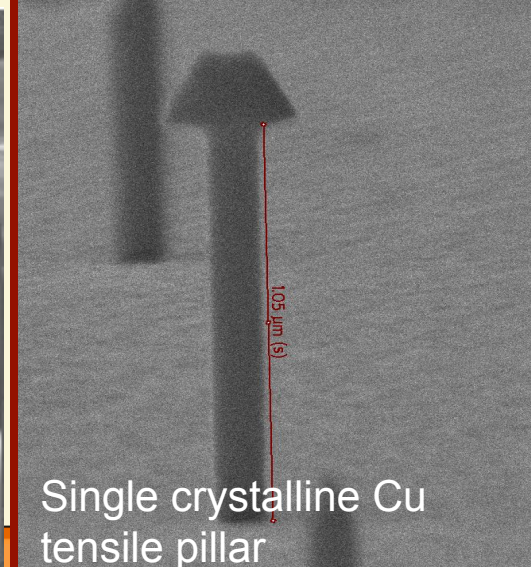
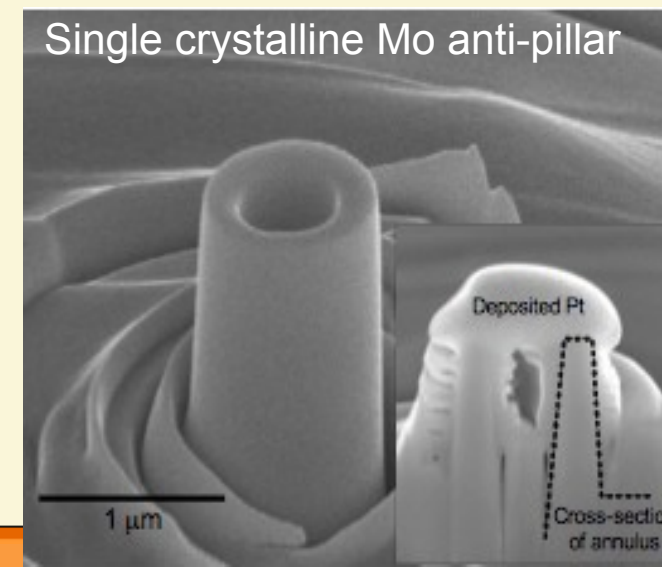
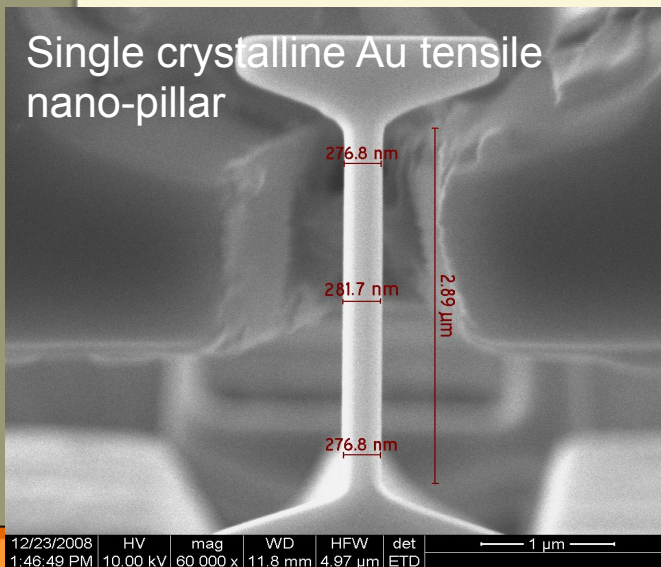
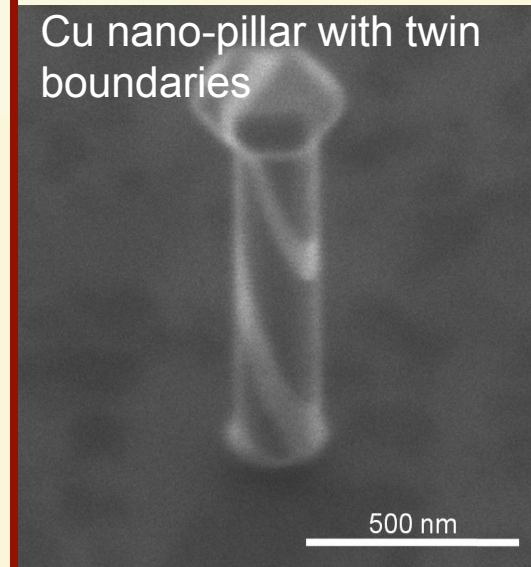
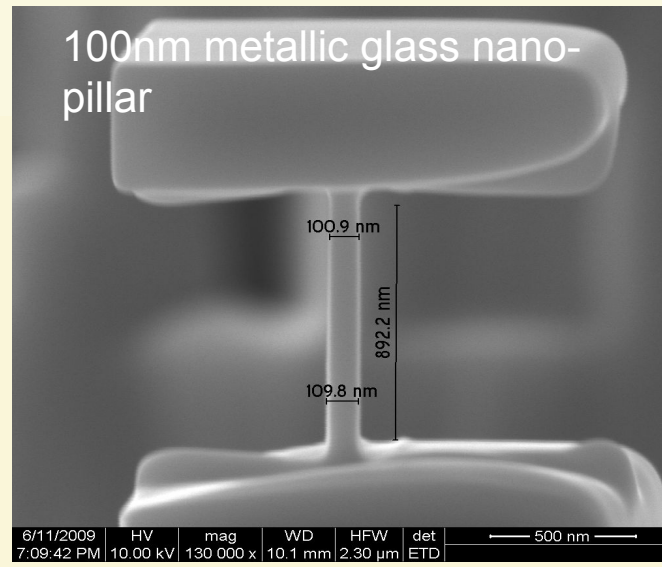
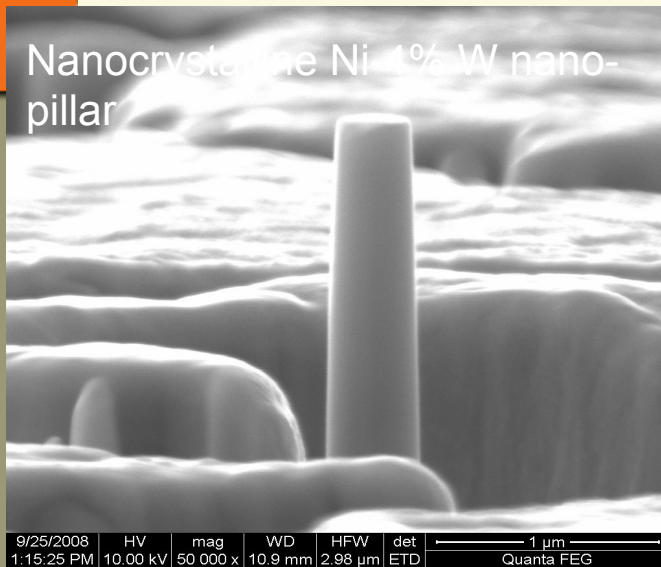
det
ETD

500 nm

Nano-pillar Fabrication Methods

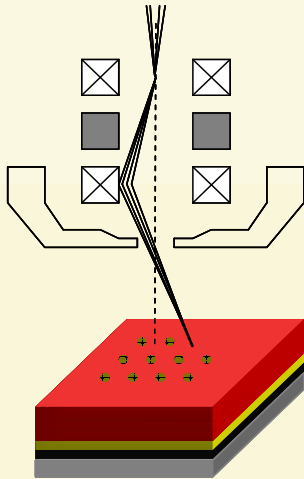
Focused Ion Beam

FIB-less

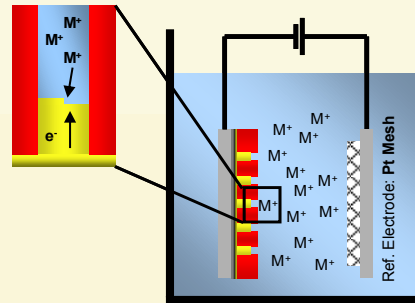


FIB-less fabrication: E-beam Litho => Electroplating

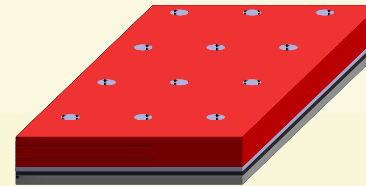
1. E-beam patterning



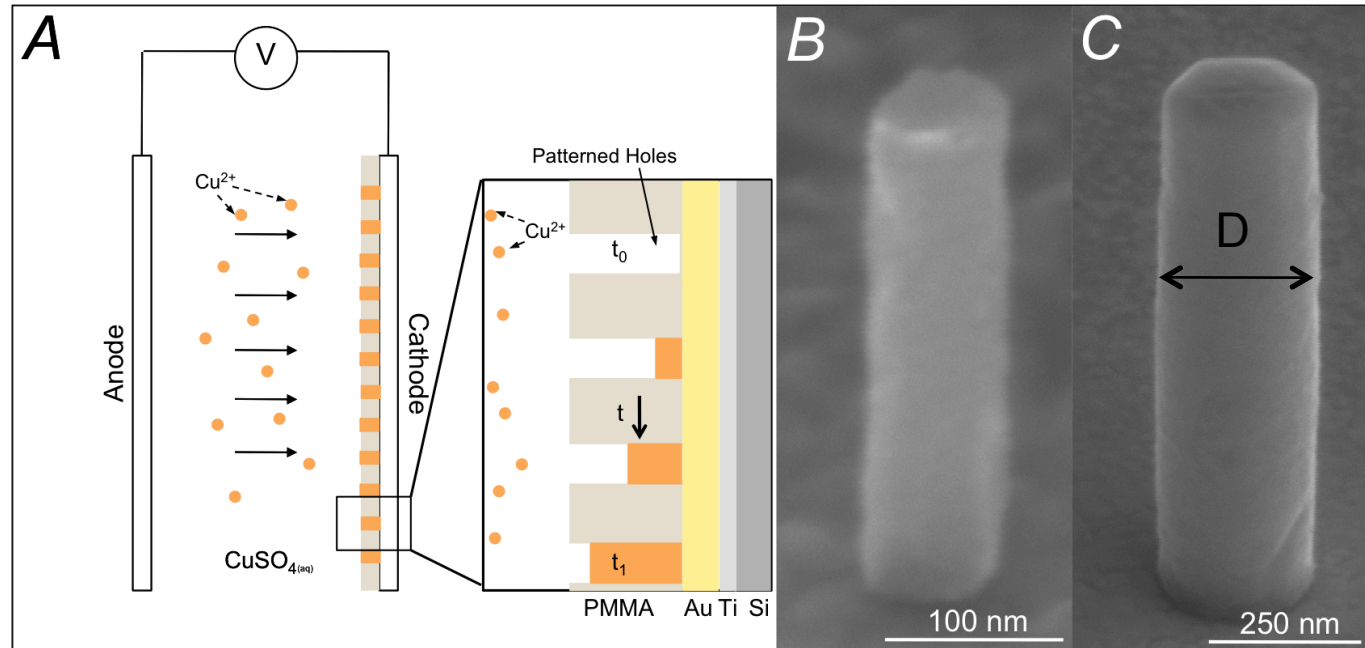
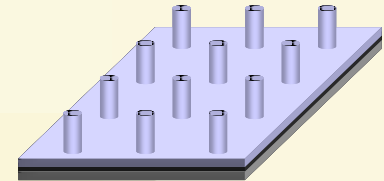
2. Electroplating



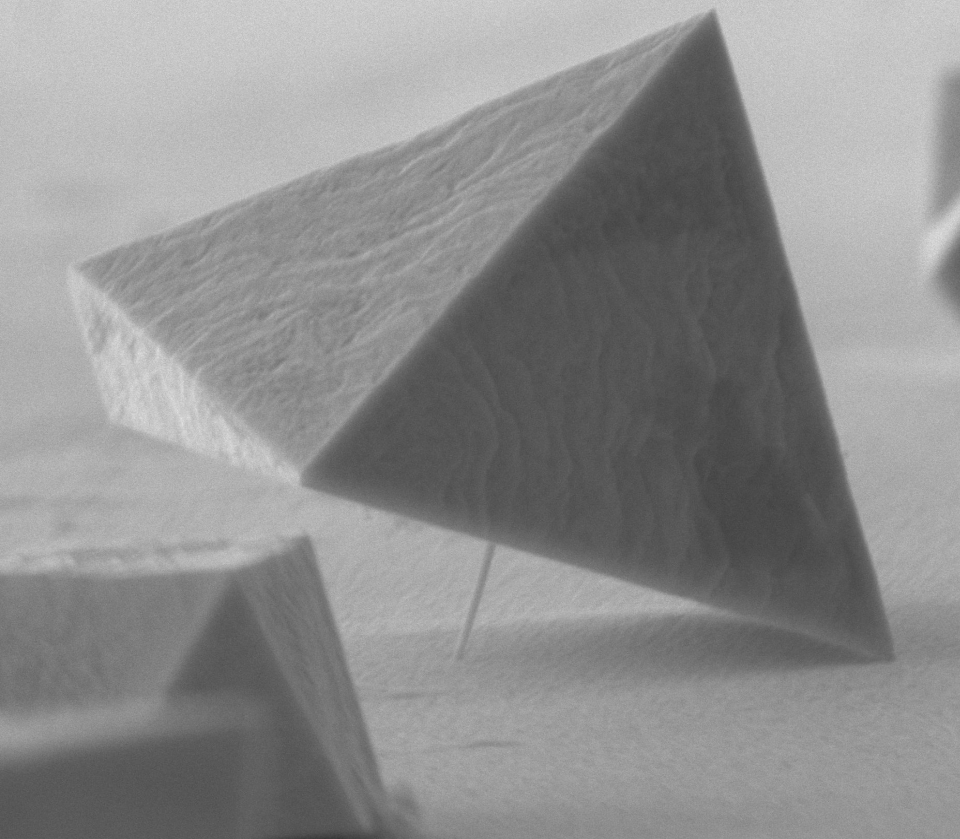
3. Pillars in PMMA Matrix



4. Free-standing pillar array



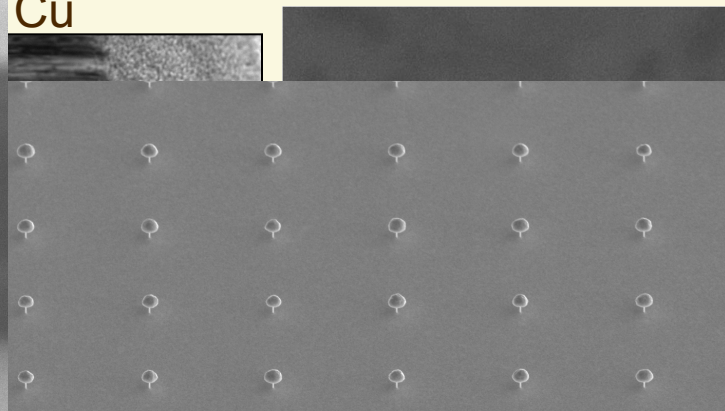
Nano-Louvre



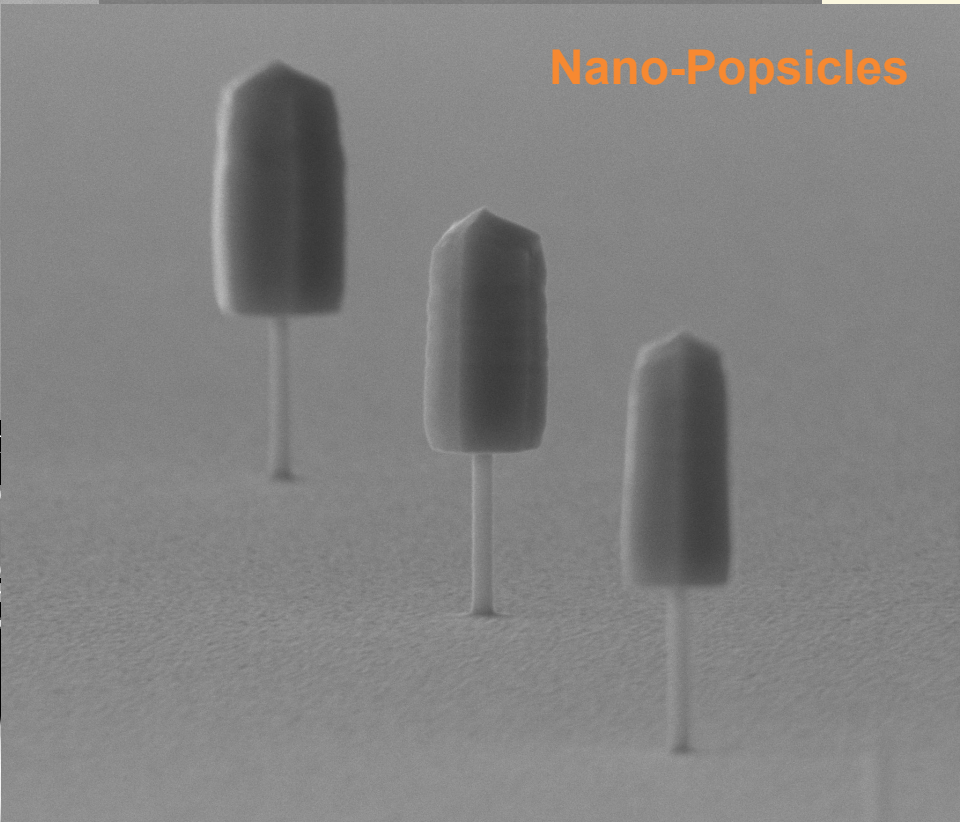
1/25/2011 HV mag WD HFW det
4:21:15 PM 10.00 kV 50 000 x 9.5 mm 5.97 μm ETD

Through Novel Synthesis

Cu



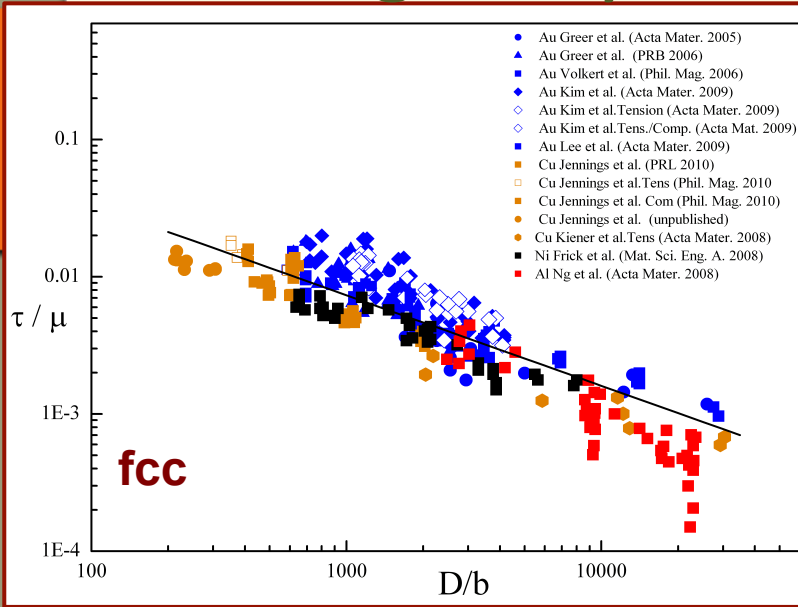
Nano-Popsicles



1/21/2011 HV mag WD HFW det
2:35:30 PM 10.00 kV 50 000 x 9.7 mm 5.97 μm ETD

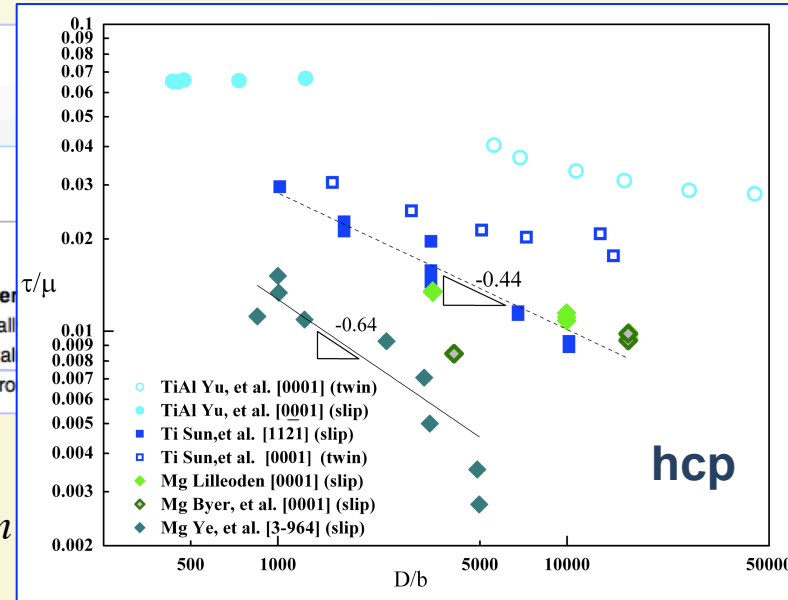
Bi-crystalline and twinned FIB-less Cu pillar

Single Crystals: Ubiquitous Size Effect

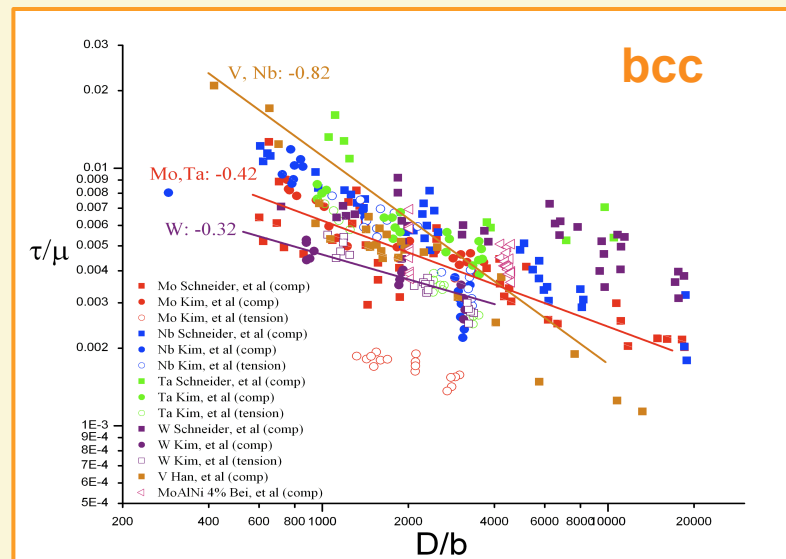


... strength (TS) or ultimate stre...
 ... contract. The UTS is usuall...
 ... intensive property, therefore its val...
 ... the temperature of the test enviro...

$$\sigma_f \propto D^{-n}$$

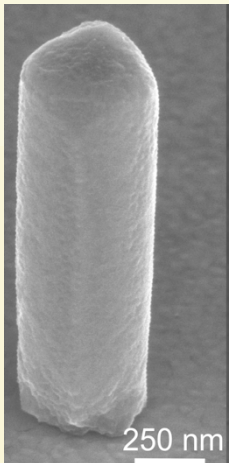


Dislocation Nucleation-controlled plasticity

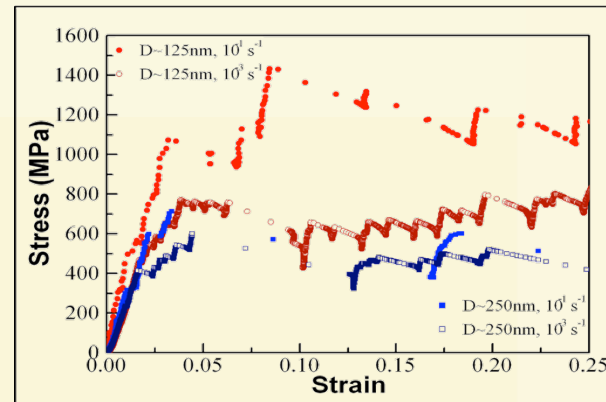
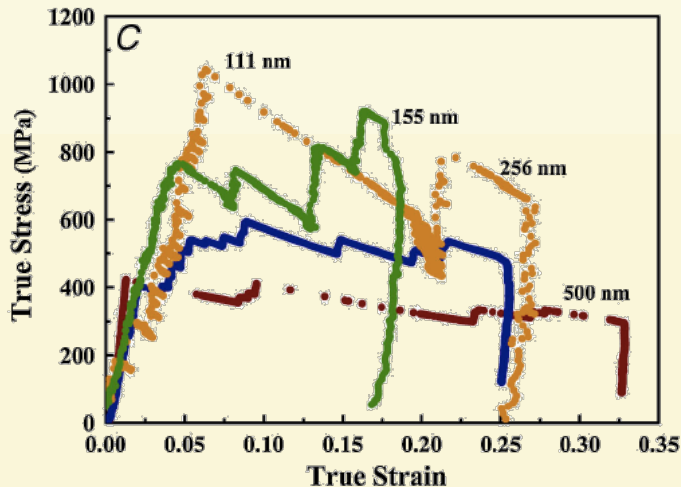
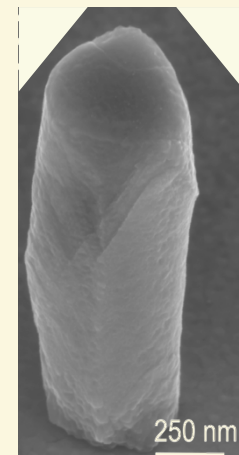


“Smaller is Stronger” and Strain Bursts

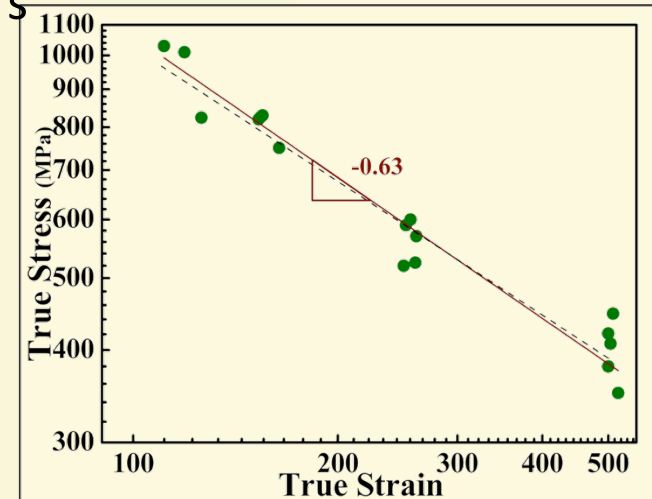
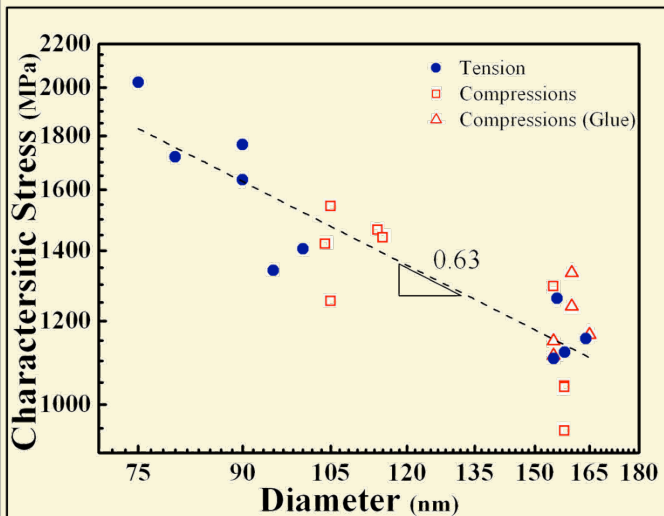
Pre-deformation



Post-deformation

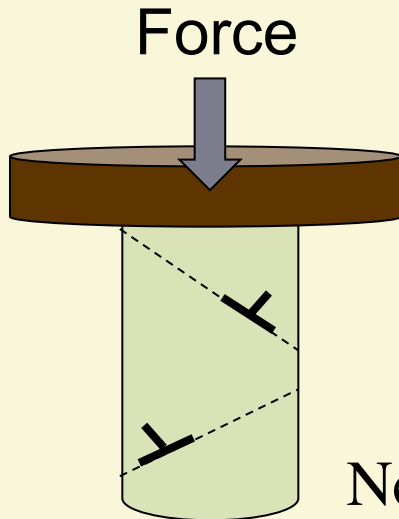
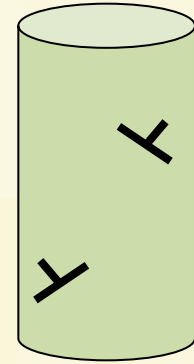


Size effects with stochastic stress-strain signature and size effects are identical to FIB-fabricated pillars



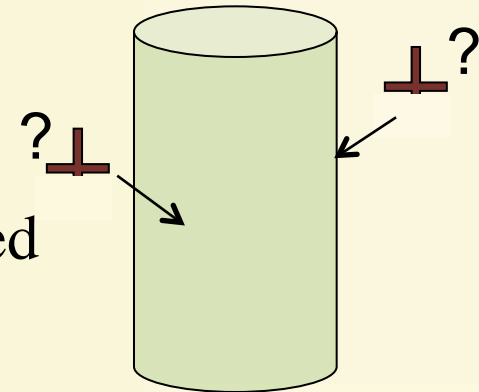
Dislocation starvation and nucleation: source-controlled plasticity

In a nano-pillar (deeply in sub-micron regime)
with non-zero initial dislocation density



Under compression dislocations leave the
crystal faster than they multiply

New dislocations have to be nucleated
WHERE?

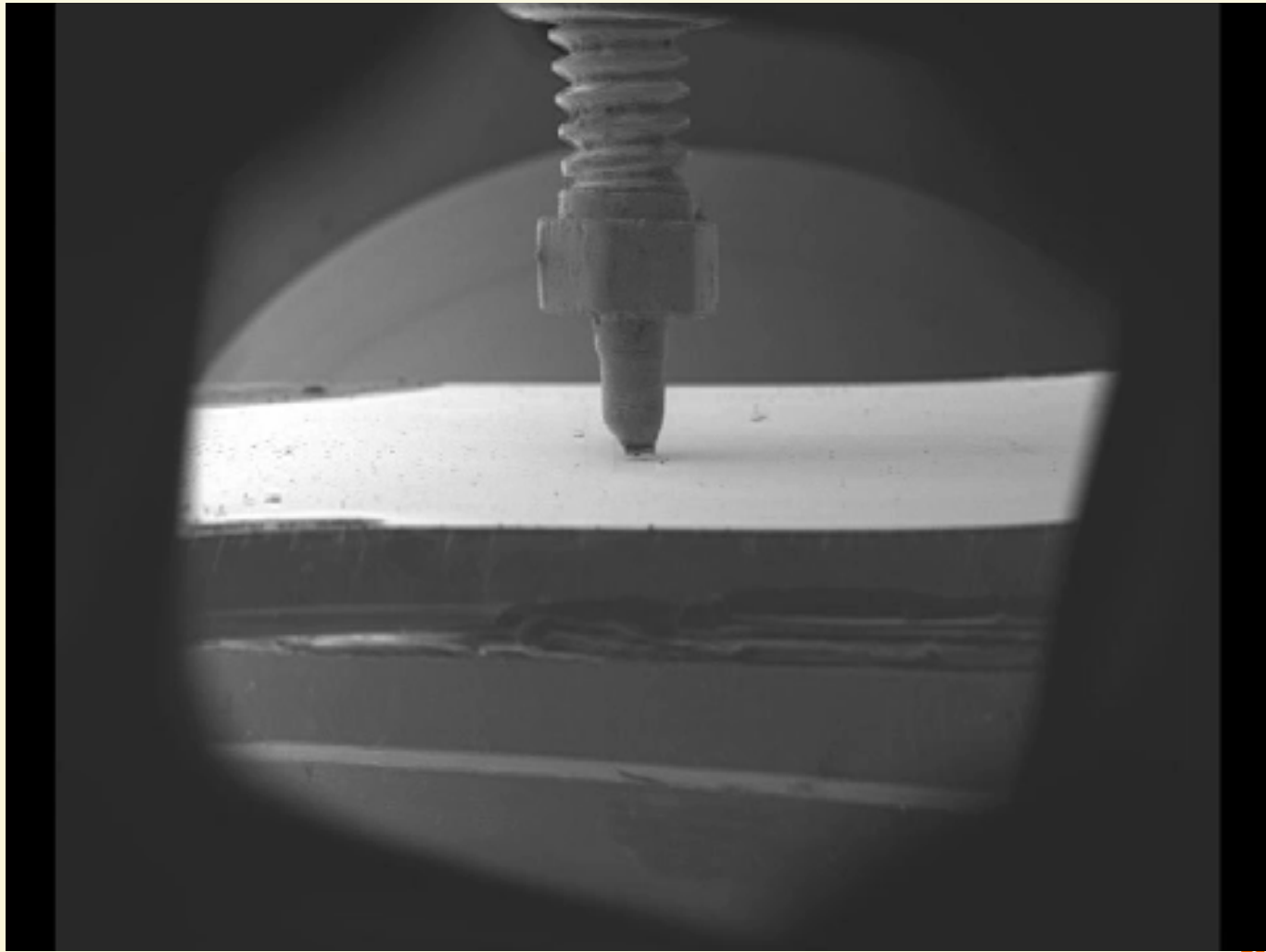


Coined **hardening by dislocation starvation**, occurs only in small
volumes and not in bulk crystals.



Insights into Deformation mechanisms: TEM

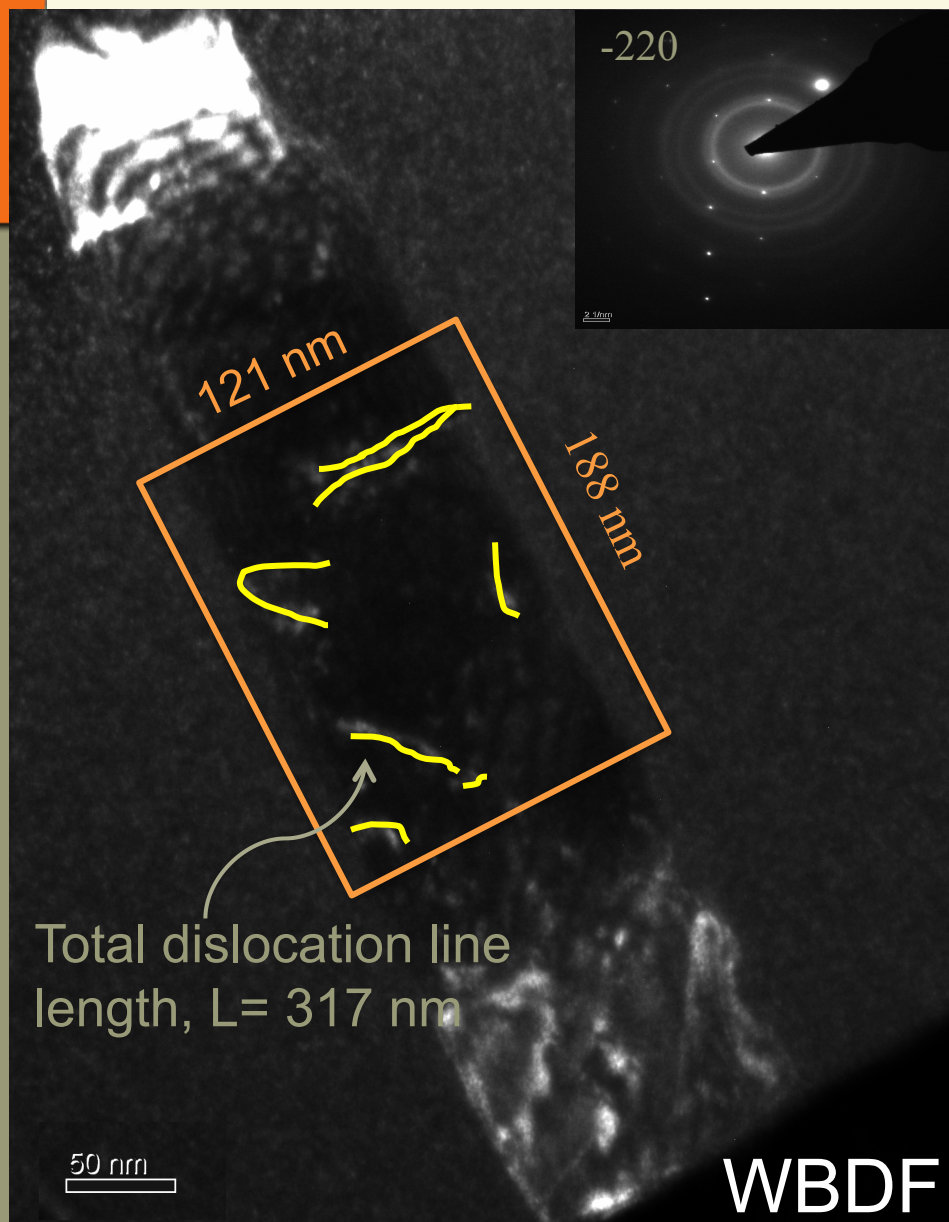
How do we TEM the same nano-pillars before and after deformation???



We test them directly on TEM grid!



Single Crystalline (FIB-less) Pillars are NOT dislocation-free



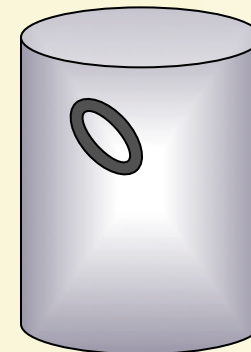
Dislocation Density:

$$\rho = L / \pi R^2 h$$

$$\rho = 1.46 \times 10^{14} \text{ m}^{-2}$$

Relatively high!

BUT important to recognize:
the lowest attainable non-zero
dislocation density is $1 \times 10^{12} \text{ m}^{-2}$

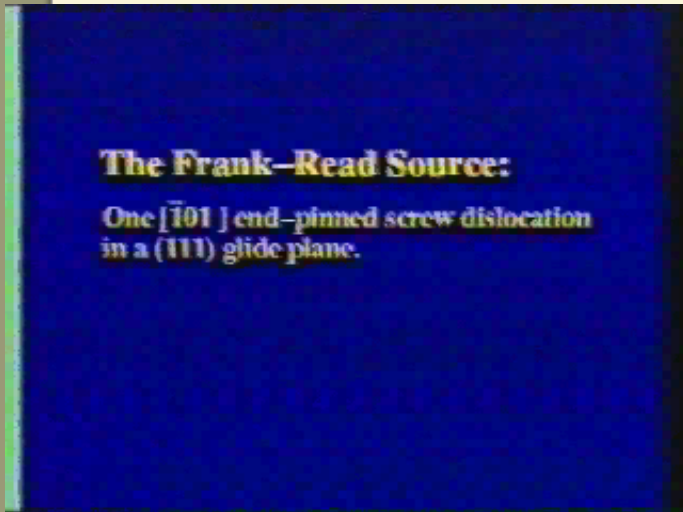


(corresponds to a 7-atom
loop in 121nm x 188 nm
cylindrical volume)

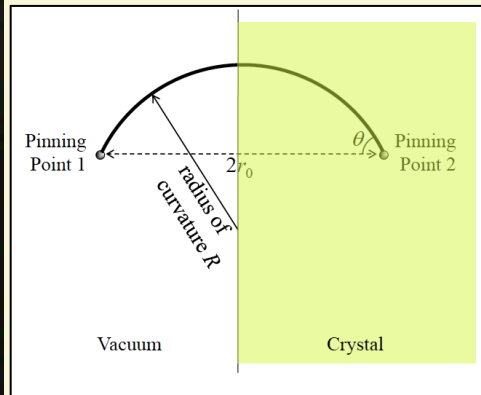


Dislocation Nucleation Sources

FRANK-READ Source
(a.k.a. conventional)
($\Omega \sim 100-1000b^3$)

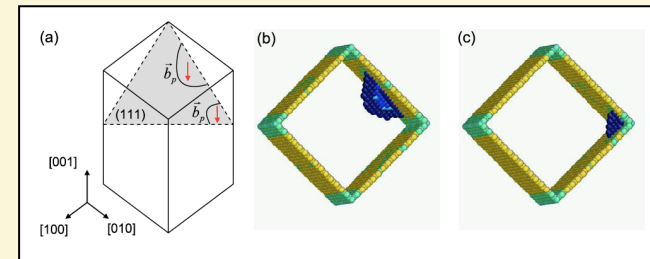


"Truncated" or SINGLE ARM Source
(micron-sized pillars)
($\Omega \sim 50-500b^3$)



Parthasarathy et al. *Scripta Mat* (2007)
Rao et al. *Acta Mat* (2008)
Tang et al *Phys Rev Lett* (2008)
Oh et al. *Nature Mat* (2009)
Weinberger et al. *Scripta Mat* (2010)

SURFACE Source
($\Omega \sim 1-10b^3$)



Gall et al *Nano Letters* (2004)
Diao et al *Acta Mat* (2006)
Zhu et al *Phys Rev Lett* (2008)
Lu et al *Nature Nano* (2010)

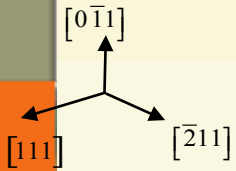
$$\Omega_{SAS} = \frac{\Omega_{F-R}}{2}$$

Activation volume can be experimentally determined by varying strain rate:

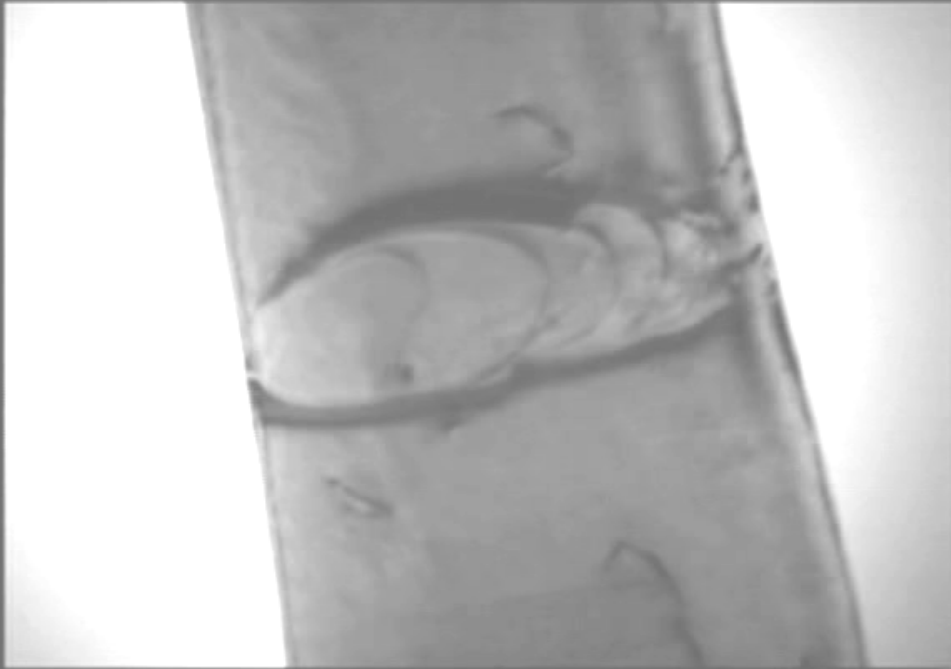
$$\Omega = k_B T \frac{\partial \ln(\dot{\gamma})}{\partial \tau}$$



Dislocation Nucleation Sources

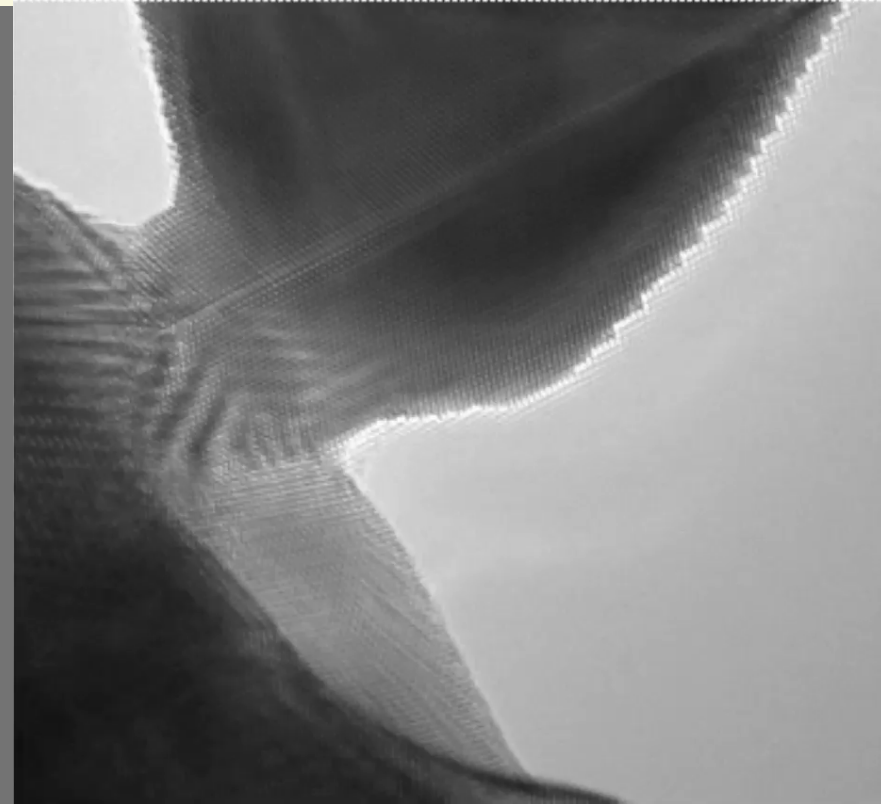


Single-arm source



(SAS TEM movie courtesy M. Legros)

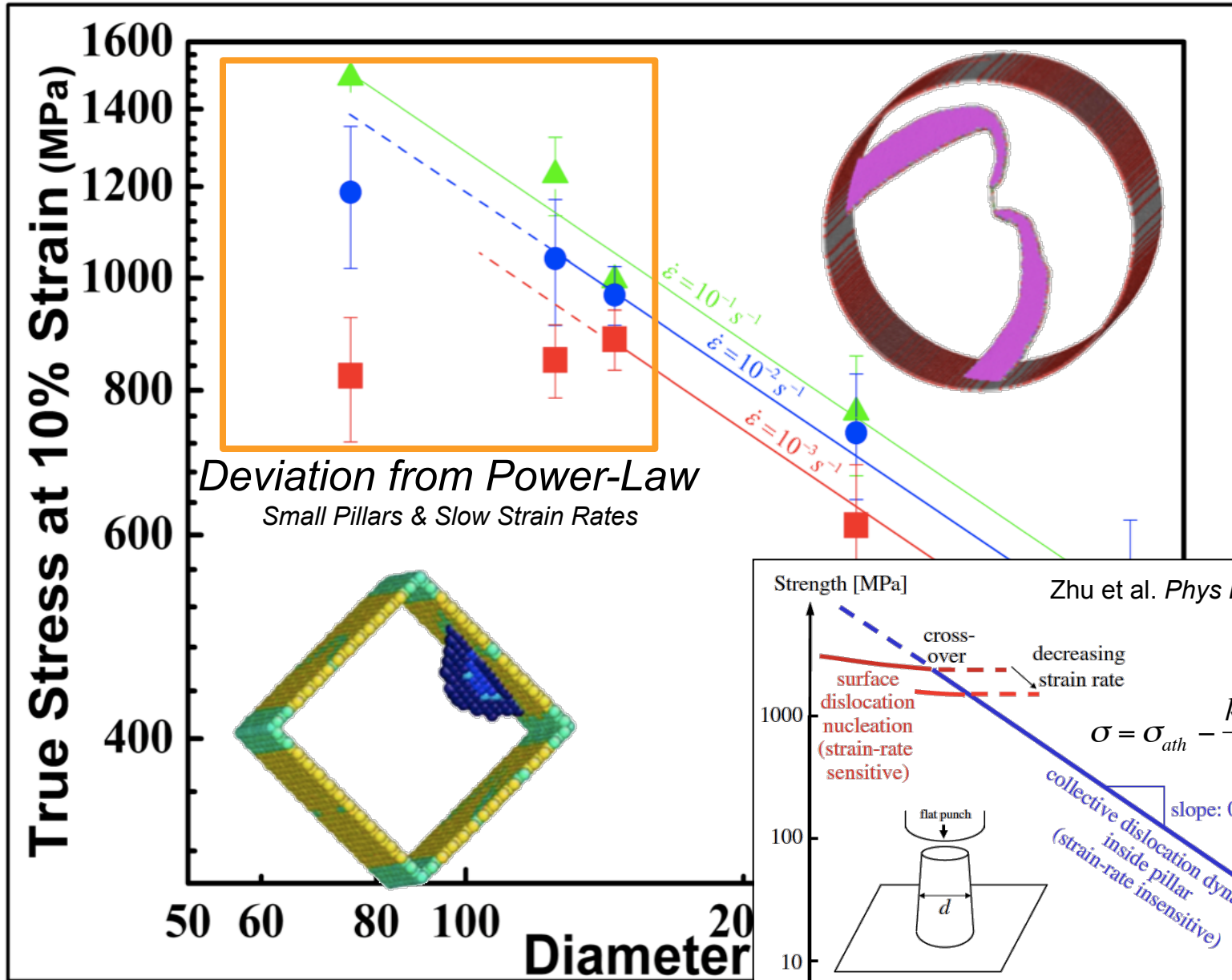
Surface source



MD movie courtesy of C. Weinberger
(SS TEM movie courtesy J. Huang)



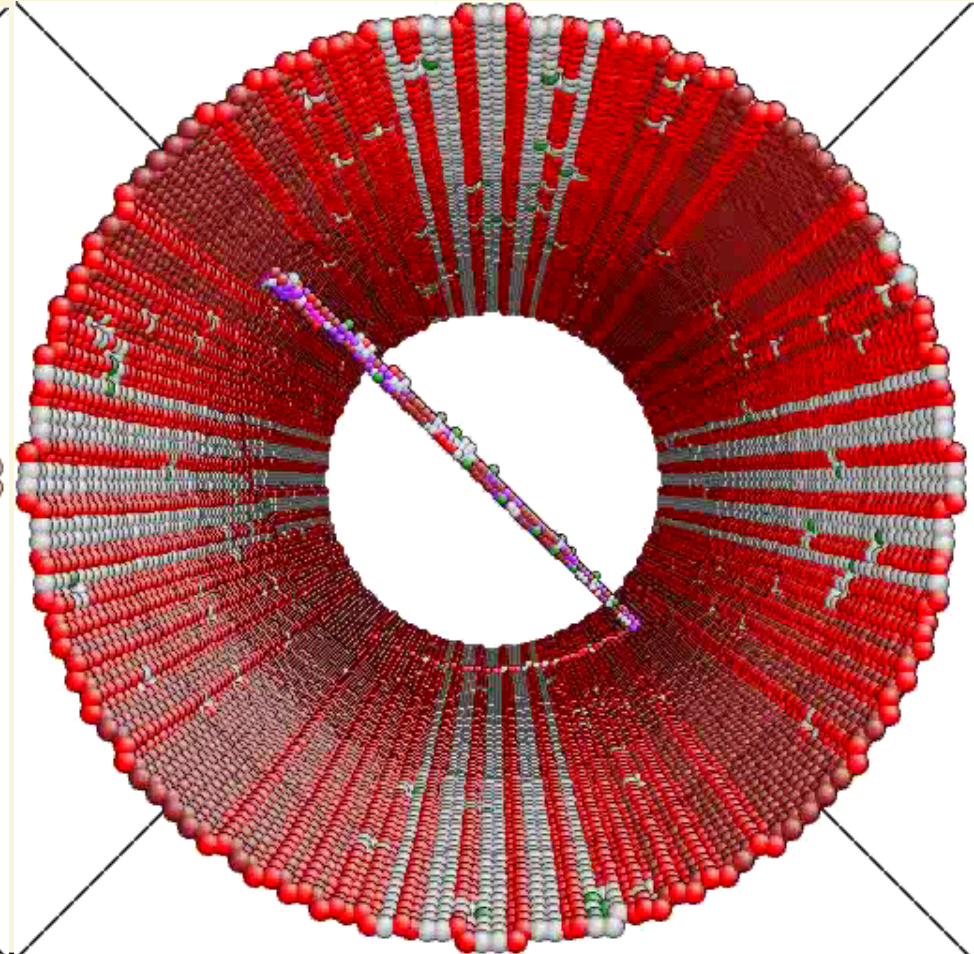
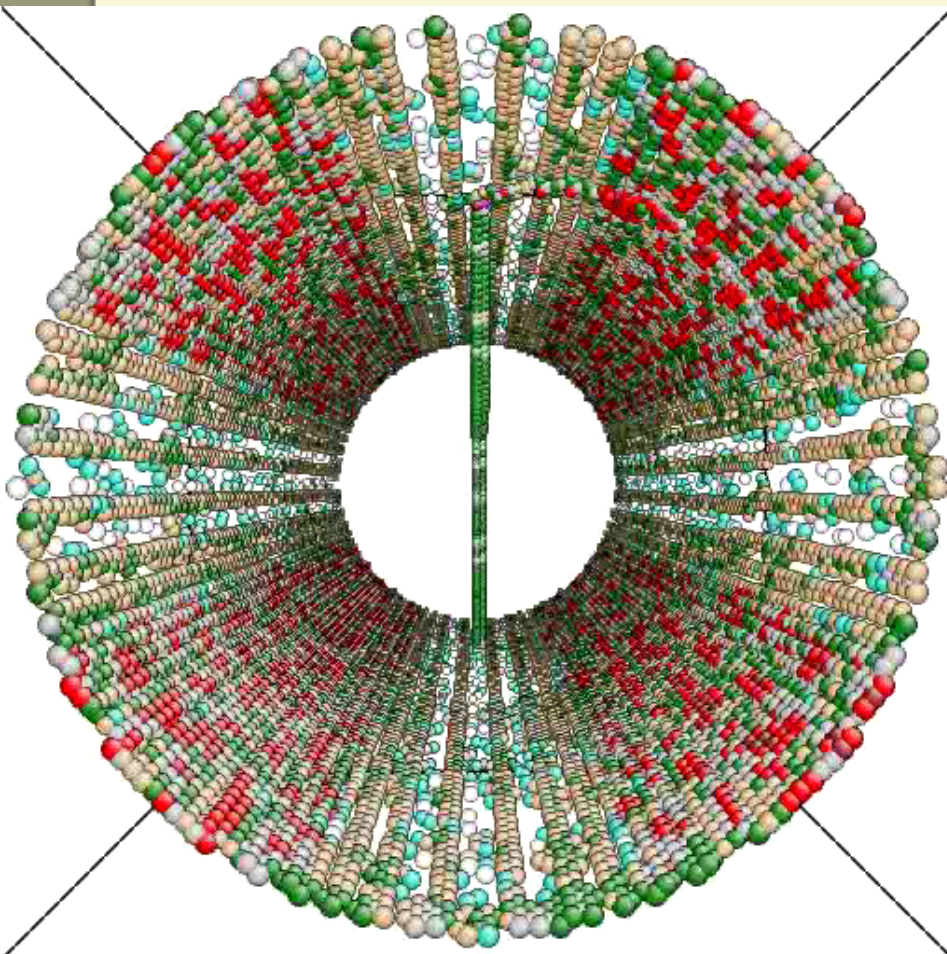
Surface vs. Single-Arm Sources



Atomistics of Dislocation Motion in Pillars: Molecular Dynamics Simulations

18nm-diameter Au pillar
Constant load = 500 MPa

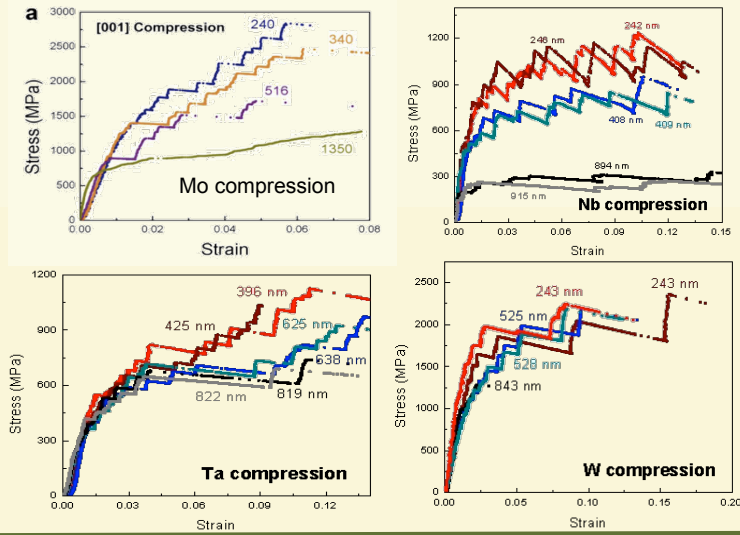
24nm-diameter Mo pillar
Constant Load = 9 GPa



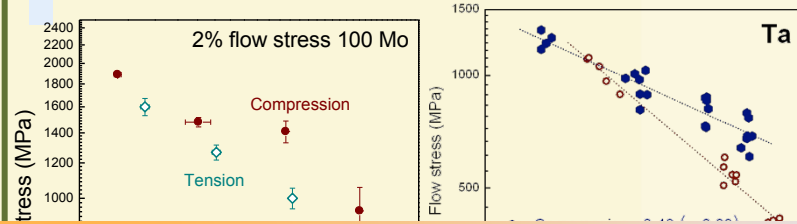
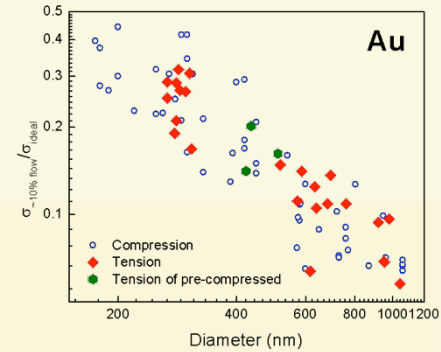
Mechanical Properties of [001] bcc nano-pillars

Stress-strain curves for Mo, Ta, Nb, and W

Compression

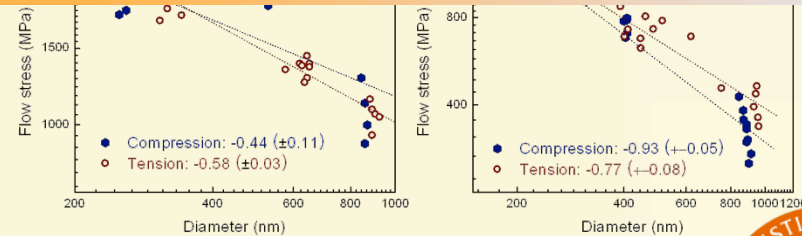
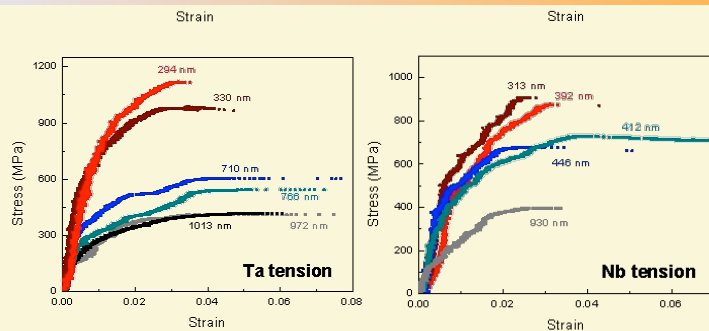


Tension vs. Compression

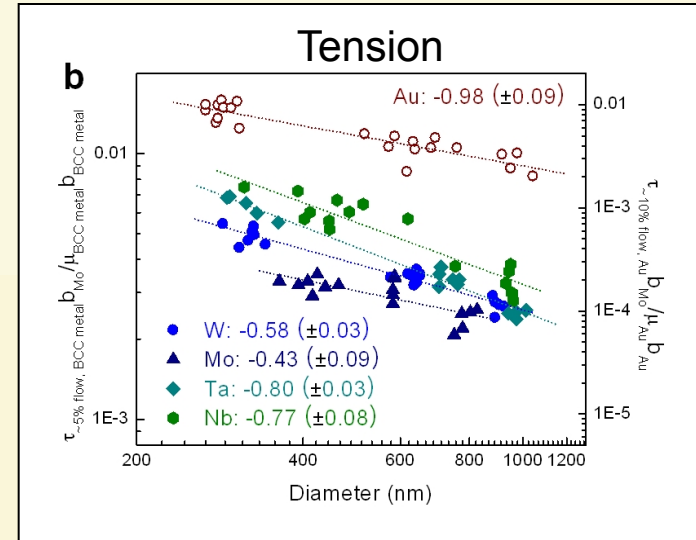
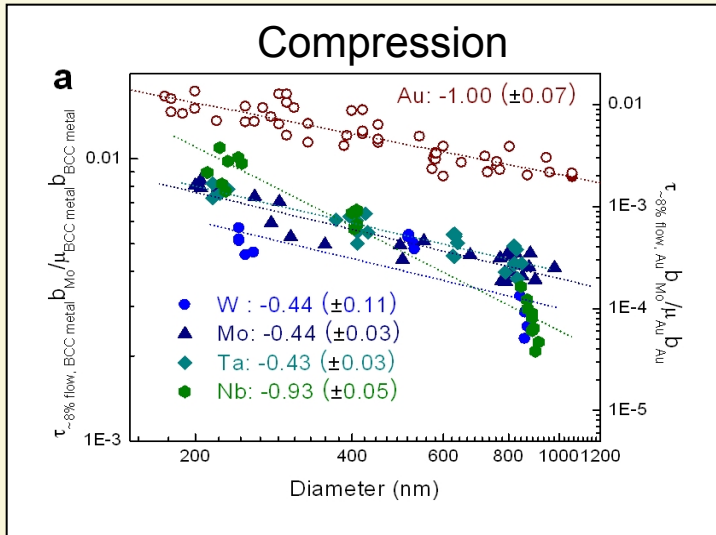


1. Stress-strain signature is stochastic, with intermittent strain bursts
2. Power-law size effects present in bcc nano structures
3. Tension-Compression asymmetry is present and is more pronounced in samples with larger diameters than smaller ones

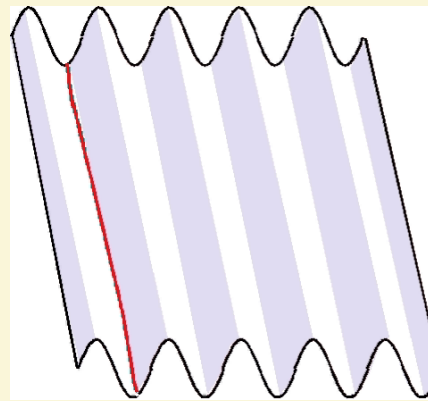
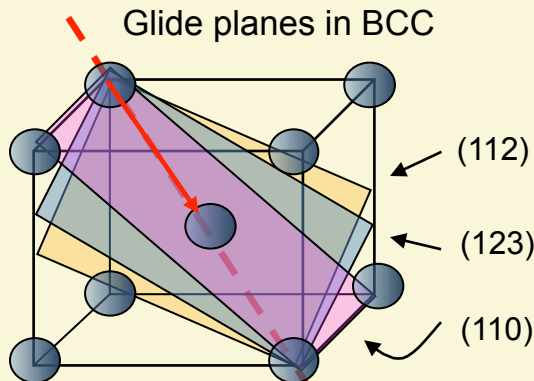
Tension



Origins of Different Size Effects

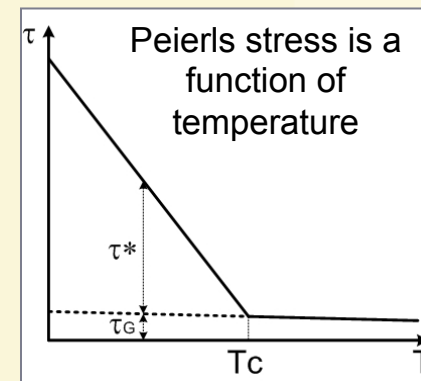


Overcoming Peierls potential is KEY in BCC Plasticity



Movie courtesy: S. Roberts

Critical temperature (K)



W: 760
Mo: 472
Ta: 440
Nb: 290

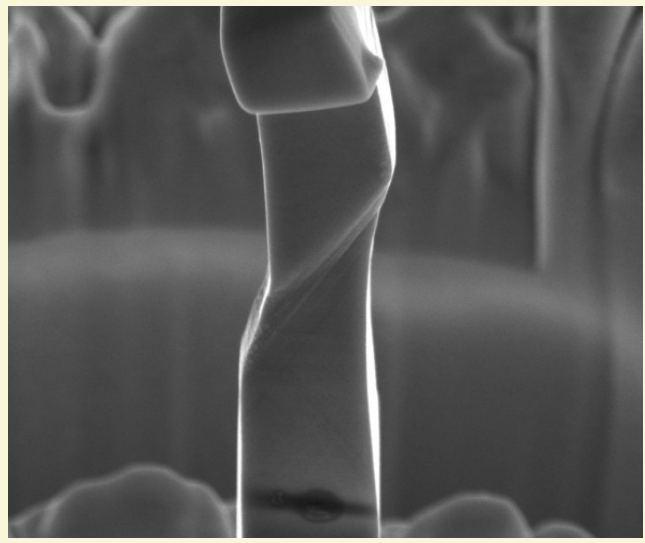
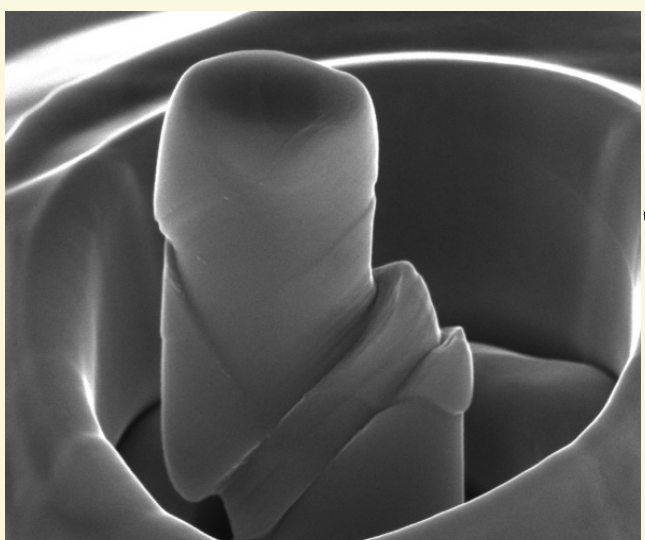
Au < Nb < Ta, Mo, W

- Dislocations propagate by kink-pair nucleation
- Must overcome Peierls potential → requires high stresses or T
- Screw dislocations are much slower than edge dislocations → dominate deformation below T_c



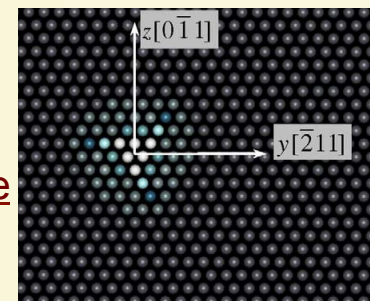
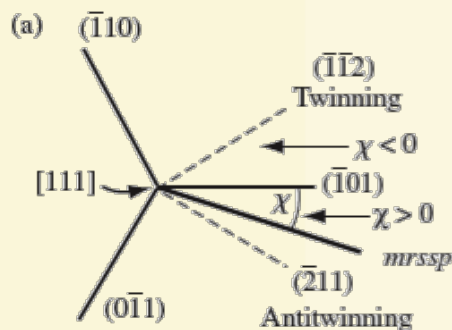
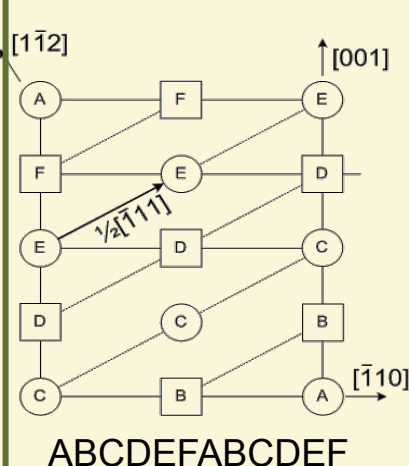
Origins of Tension-Compression Asymmetry

Different gripping constraints



1. Intrinsic effect of BCC structure

- Shear stresses in positive and negative $\langle 111 \rangle$ are not equivalent (except on $\{110\}$ planes)
- Twinning vs. Anti-twinning on $\{112\}$ planes (not mirror)



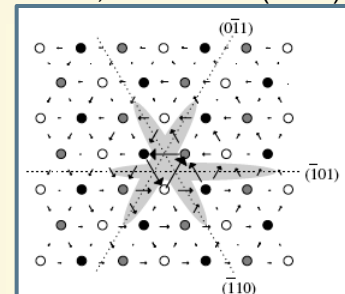
Tian and Woo, *MSE and A* (2004)

2. Extrinsic effect of BCC structure

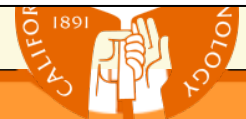
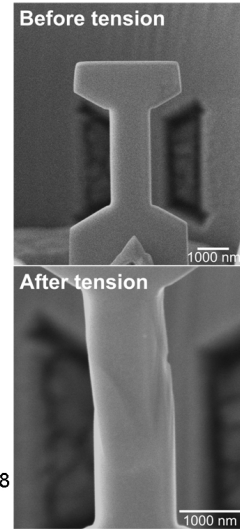
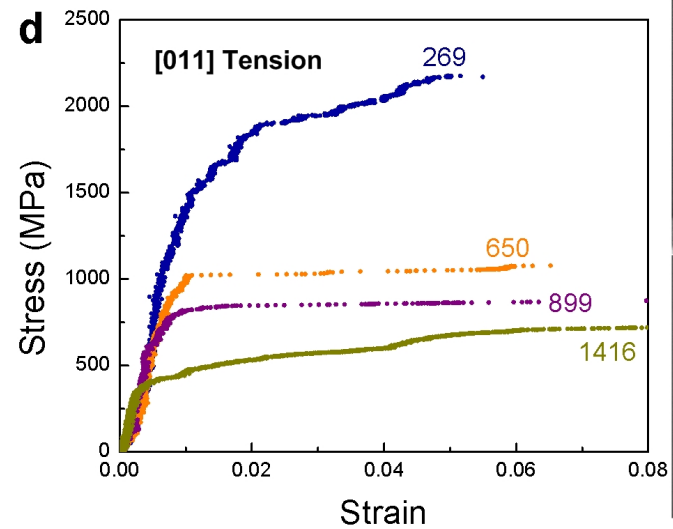
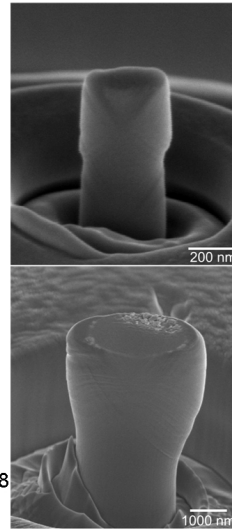
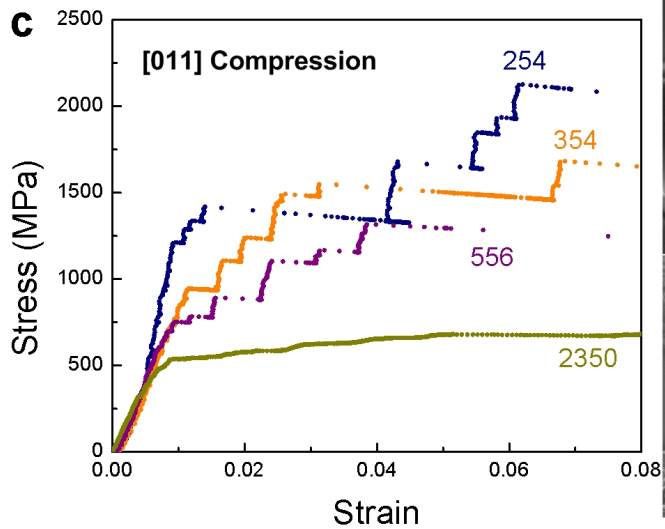
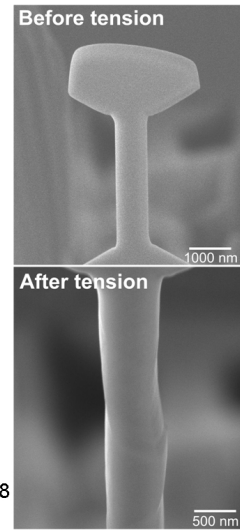
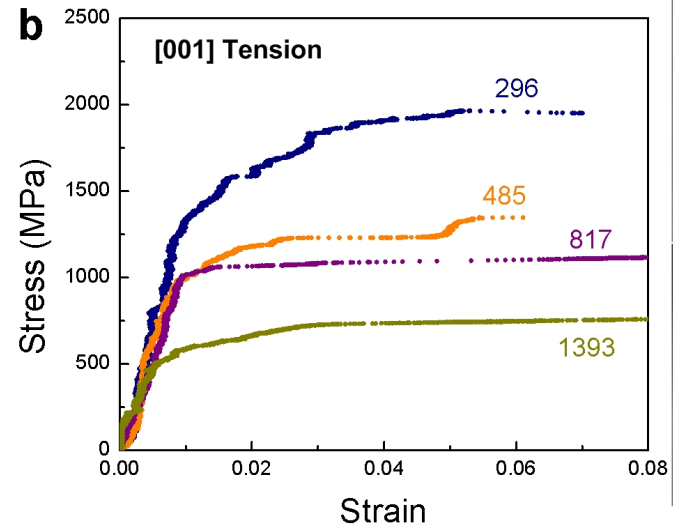
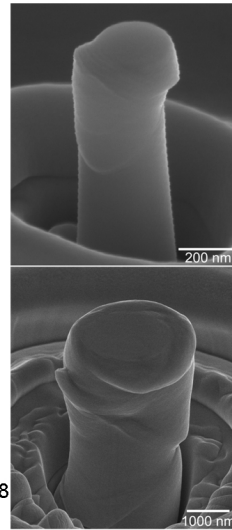
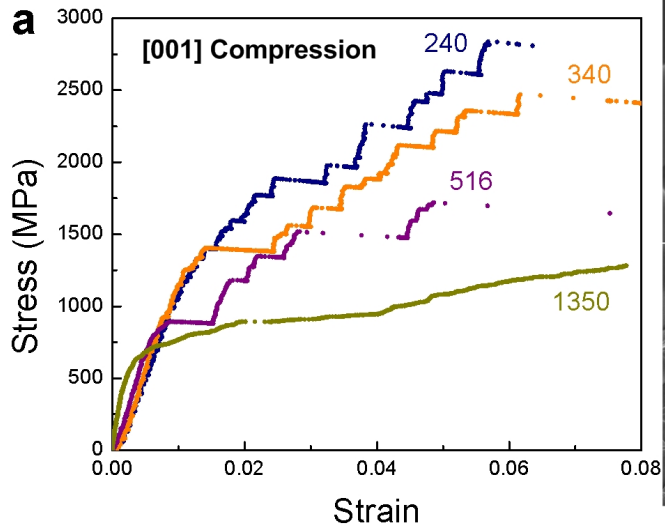
- Non-planar screw dislocation cores
- Non-Schmid behavior: Importance of shear stress components perpendicular to slip direction:

“+” for tension $\rightarrow \tau_p \downarrow \rightarrow CRSS \downarrow$

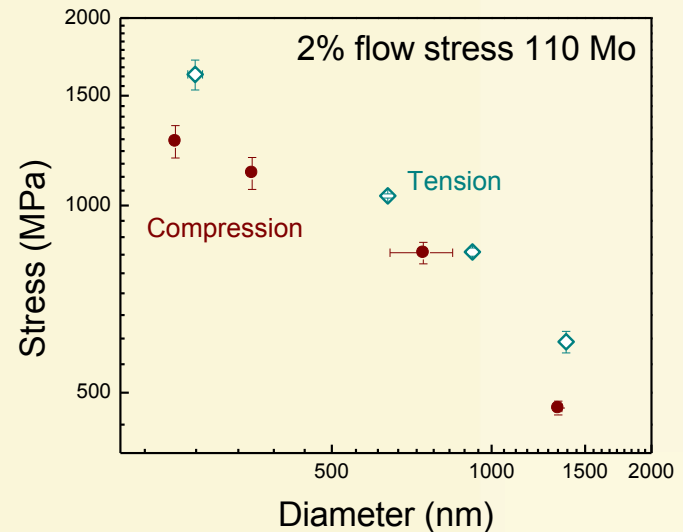
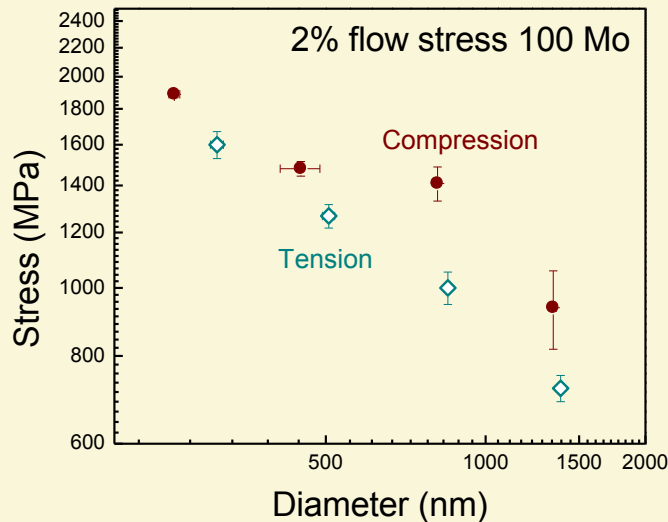
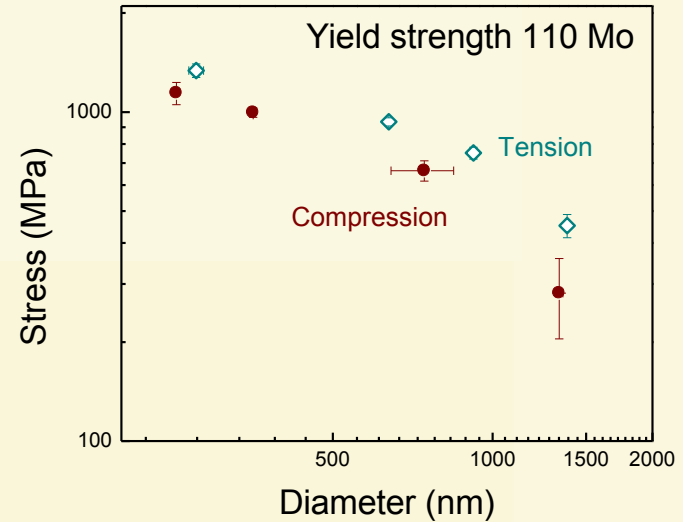
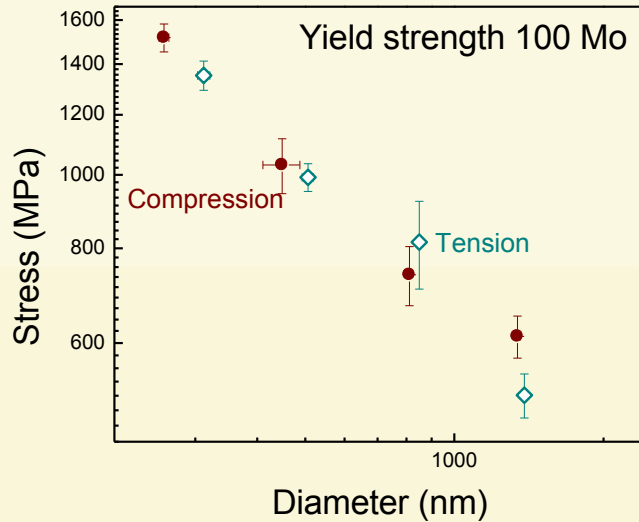
“-” for compression $\rightarrow \tau_p \uparrow \rightarrow CRSS \uparrow$



Effects of Crystallographic Orientation: [001] vs. [011]



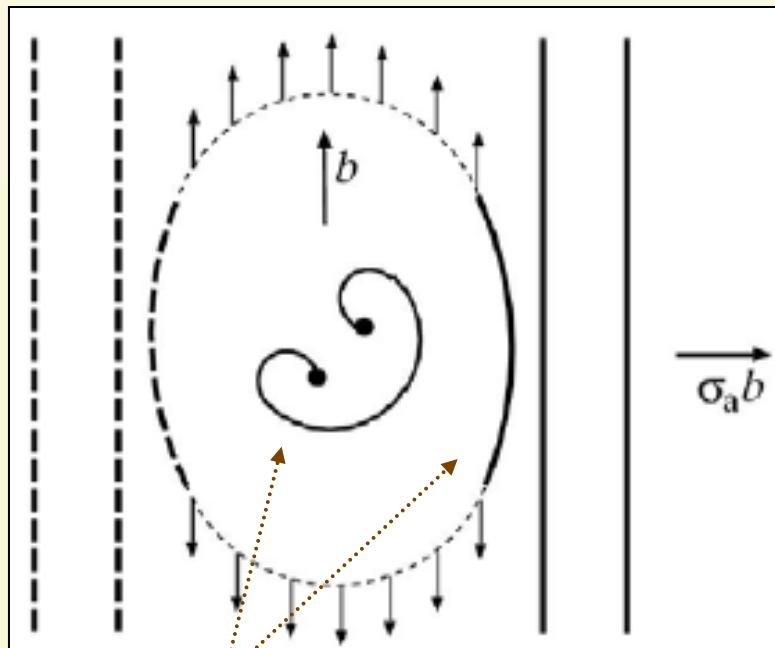
Effect of Orientation: [001] vs. [011]



Tension-compression asymmetry is more pronounced in **flow stress** (rather than in yield strength) and in samples with **larger diameters** (rather than smaller ones)

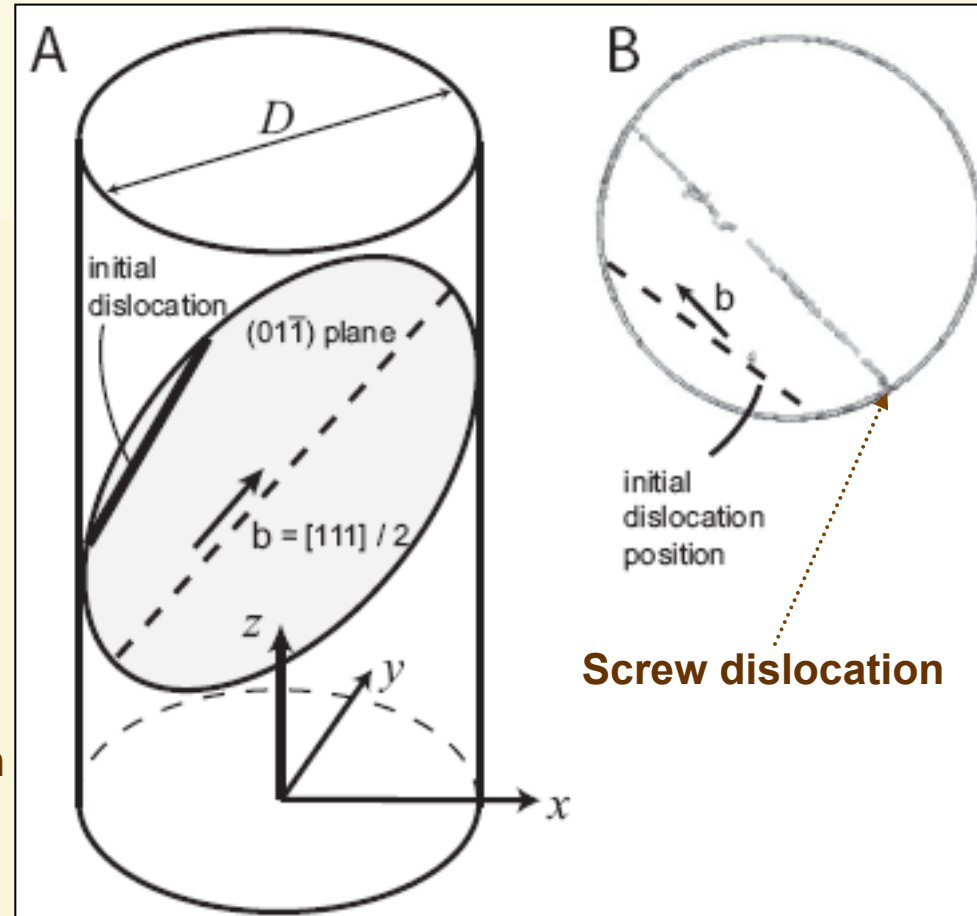


Diminishing effects of screw dislocations with smaller size



Mixed dislocation

Screw dislocation

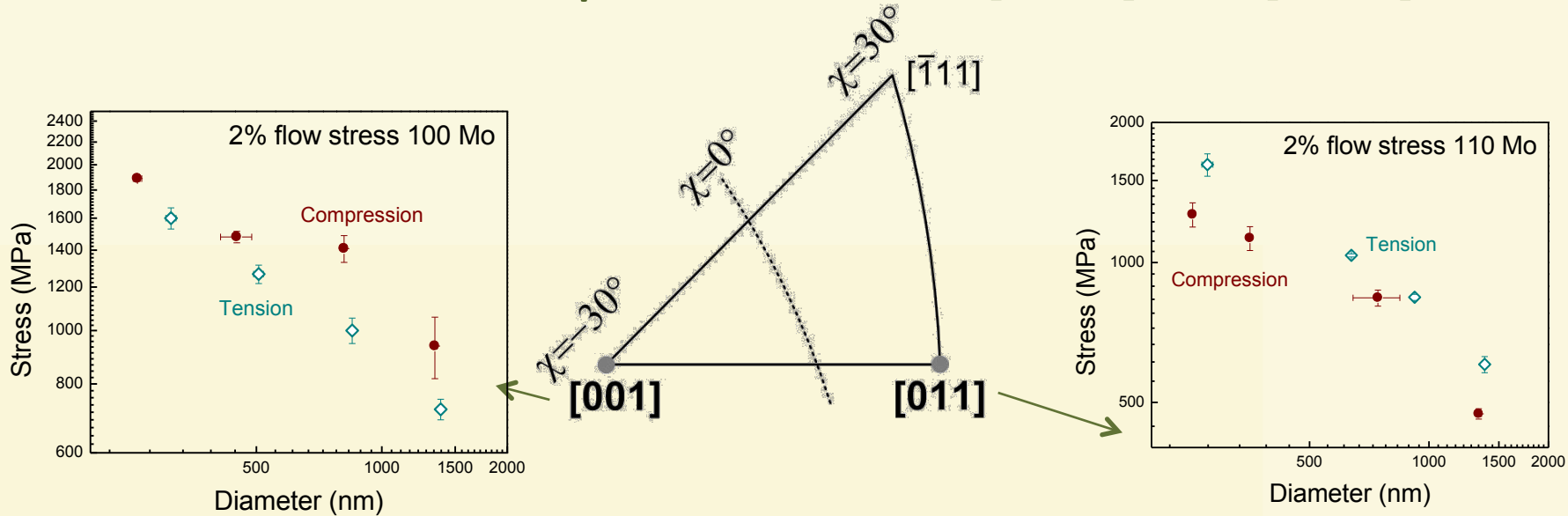


Screw dislocation

Screw dislocations appear to play a more important role in **flow stress** (rather than yield stress) and in **larger** (rather than smaller) pillars



Tension vs. Compression and [001] vs. [011]



Orientation Factor	Slip System	Schmid
[001]	(1 01)[111]	0.41
	(-211)[111]	0.24
	(-1-12)[111]	0.47
[011]	(-211)[111]	0.47
	(-1-12)[111]	0.24

Opposite χ for $(\bar{1}\bar{1}2)$ and $(\bar{2}11)$ planes \Rightarrow diametrically opposite twinning-antitwining slip

- [001] orientation: $(\bar{1}\bar{1}2)$ shears in the **twinning** sense \Rightarrow **Compression** > **Tension**
- [011] orientation: $(\bar{2}11)$ shears in the **antitwining** sense \Rightarrow **Tension** > **Compression**

**Compression > Tension for [100] Mo while
Tension > Compression for [110] Mo**



Deformation Mechanisms and Size Effects

Plasticity carriers:
Dislocations

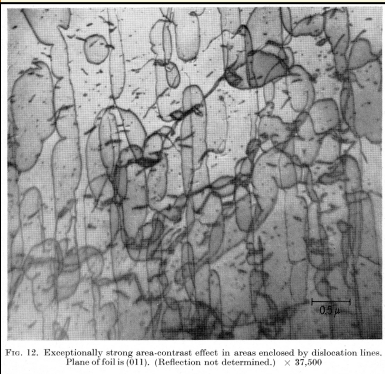


FIG. 12. Exceptionally strong area-contrast effect in areas enclosed by dislocation lines. Plane of foil is (011). (Reflection not determined.) $\times 37,500$

Low and Trial, *Acta Met.* (1962)
Fe-3% Si

Single Crystals
(Au, Mo, Nb, etc.)

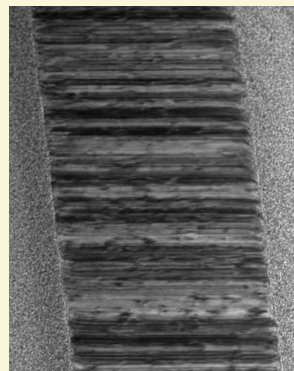
Plasticity carriers:
Dislocations + grain/twin boundaries

$\{h_1, k_1, l_1\}$ $\{h_2, k_2, l_2\}$

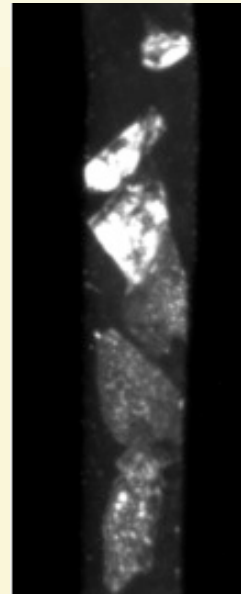


Bi-Crystals (Al)

See poster by **A. Kunz**
(Room 31B)

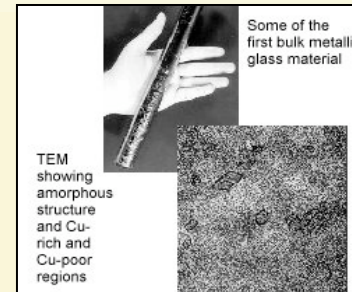


Nano-twinned
Metals (Cu)



Nanocrystalline
Metals (Ni)

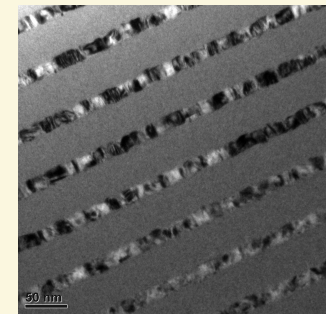
Plasticity carriers:
**Shear Transformation
Zones (STZs)**



Metallic glasses

See talk by **D. Jang**
on Thursday at 2pm
(Bulk Metallic Glasses VIII)

Plasticity carriers:
STZs + dislocations



**Amorphous/
Nanocrystalline
Nanolaminates**

See talk by **J.-Y. Kim**
on Thursday at 2:20pm
(1-D Mechanics)

Increasing disorder (introducing boundaries and amorphous-ness)



Summary and Acknowledgements

- Single crystalline Cu (fcc) nano-pillars fabricated without FIB yet with similar dislocation densities exhibit an identical size effect and stochastic intermittent flow as FIB-produced ones
- Dislocation starvation followed by surface source nucleation likely dominates plasticity at sizes below $\sim 125\text{nm}$
- Dislocation multiplication through single-arm source operation likely governs plasticity in pillars above $\sim 125\text{nm}$ diameters
- Single crystalline Cu nano-pillars exhibit significant strain rate sensitivity at very small sizes, possibly corresponding to activation of surface sources
- Body-centered (bcc) nano-pillars also exhibit stochastic behavior, but much more complex size effects and tension-compression asymmetry

Helpful discussions:

C. Weinberger (Sandia NL)
J. Li (U Penn)



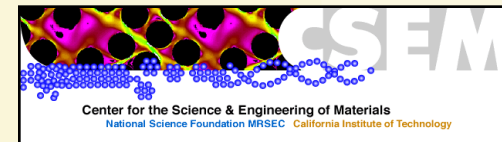
Award No: N000140910883



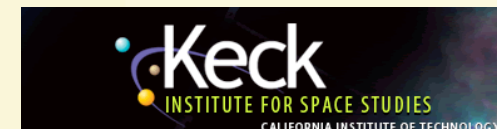
DARPA Young Faculty
Award



NSF Career Grant DMR-0748267



DMR-0520565

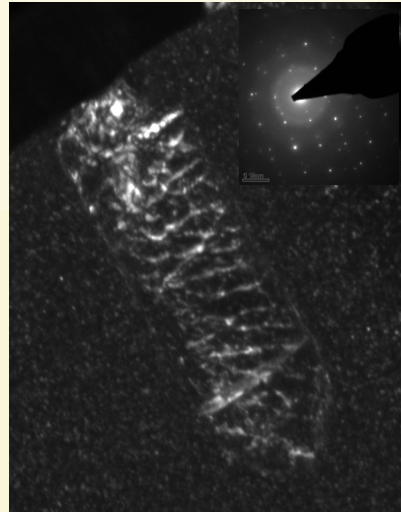
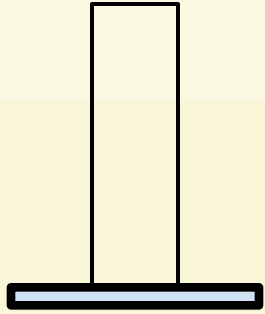


For details/publications: <http://jrgreer.caltech.edu/>

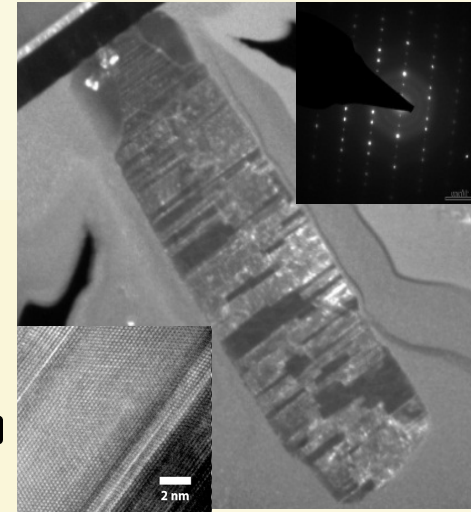
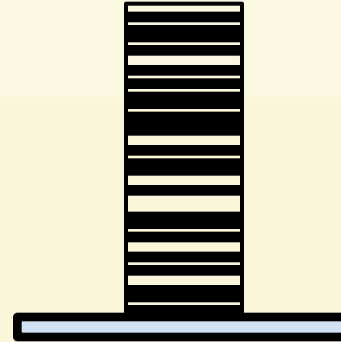


Introducing multiple boundaries

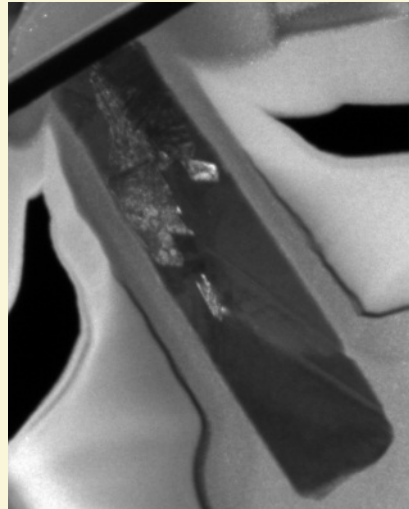
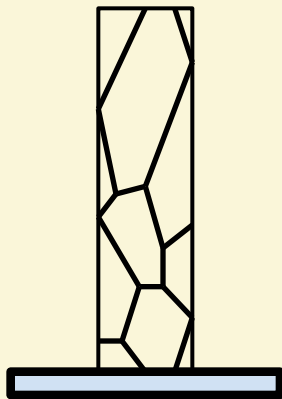
Single Crystals



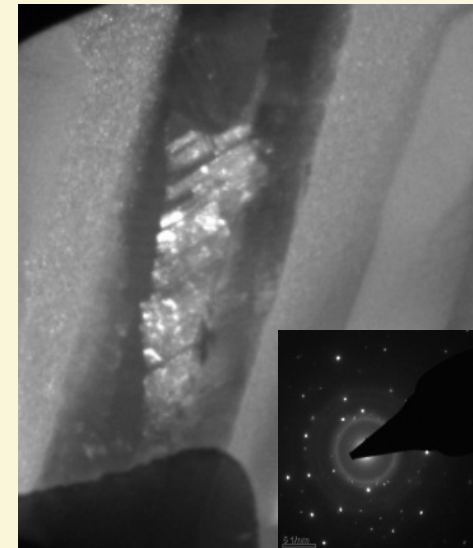
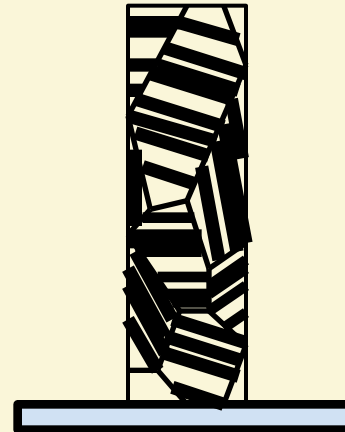
Nano-twinned



Nanocrystalline

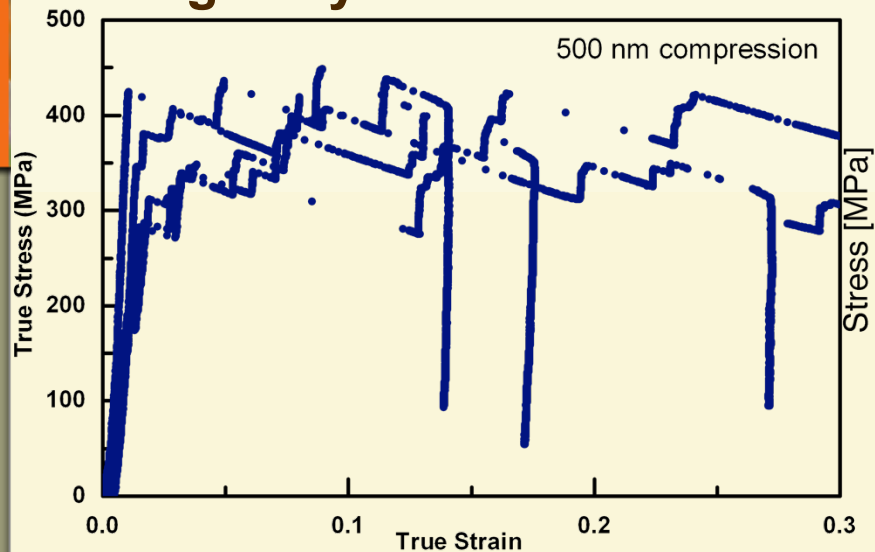


Nanocrystalline + Nano-twinned

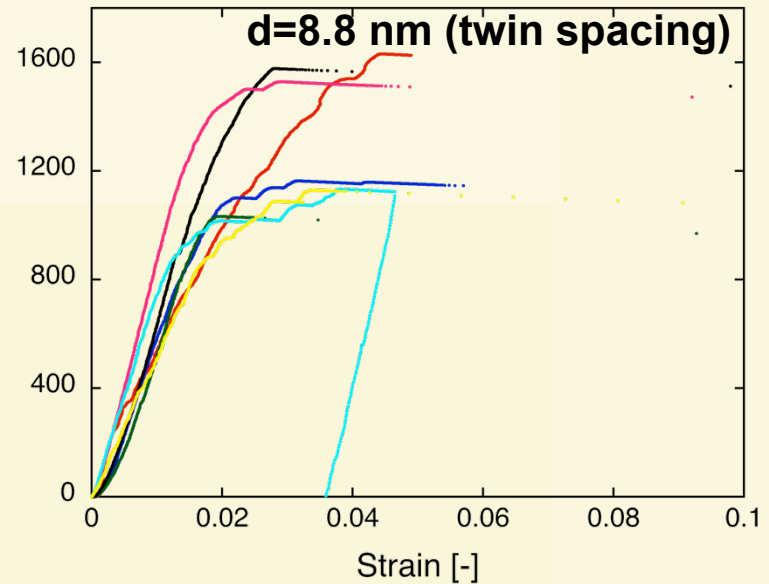


Stress vs. strain for each microstructure (D=500nm)

Single crystalline

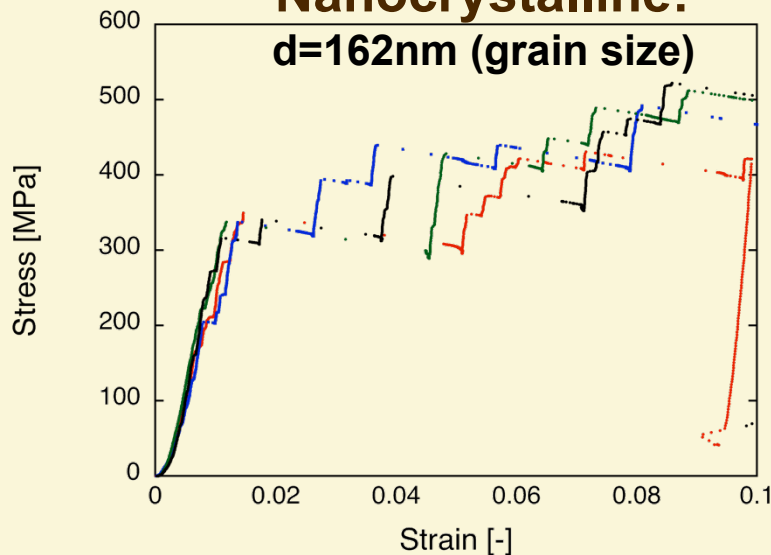


Nano-twinned:



Nanocrystalline:

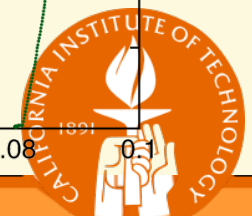
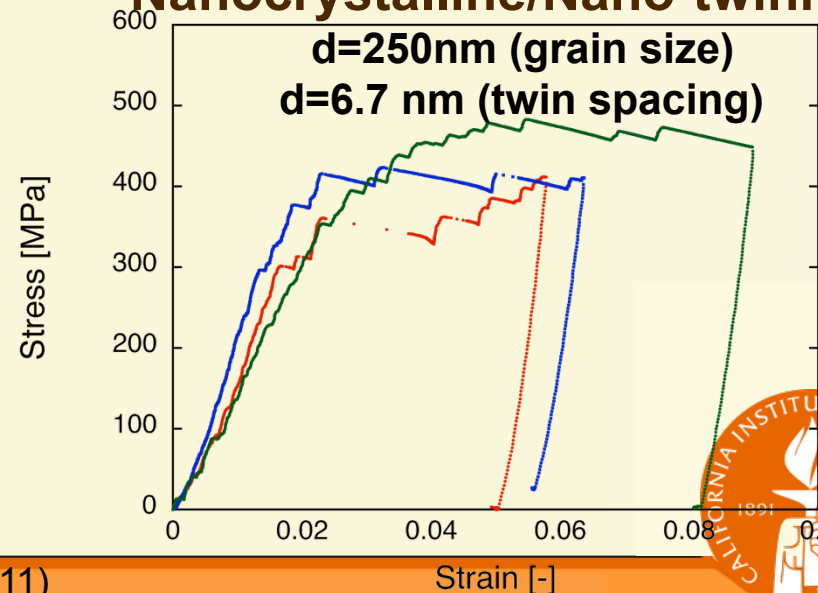
$d=162$ nm (grain size)



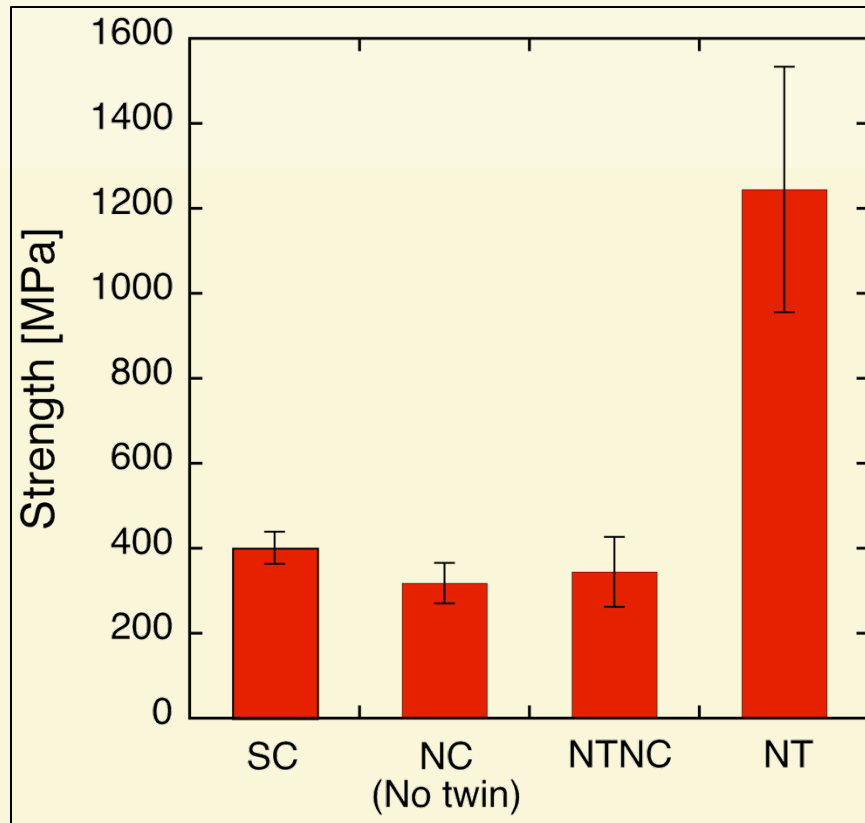
Nanocrystalline/Nano-twinned:

$d=250$ nm (grain size)

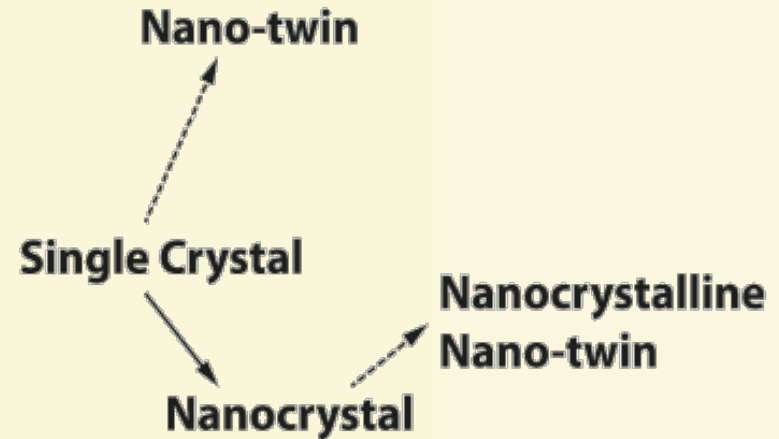
$d=6.7$ nm (twin spacing)



Strength: Intrinsic (d) vs. Extrinsic (D)



Increasing strength

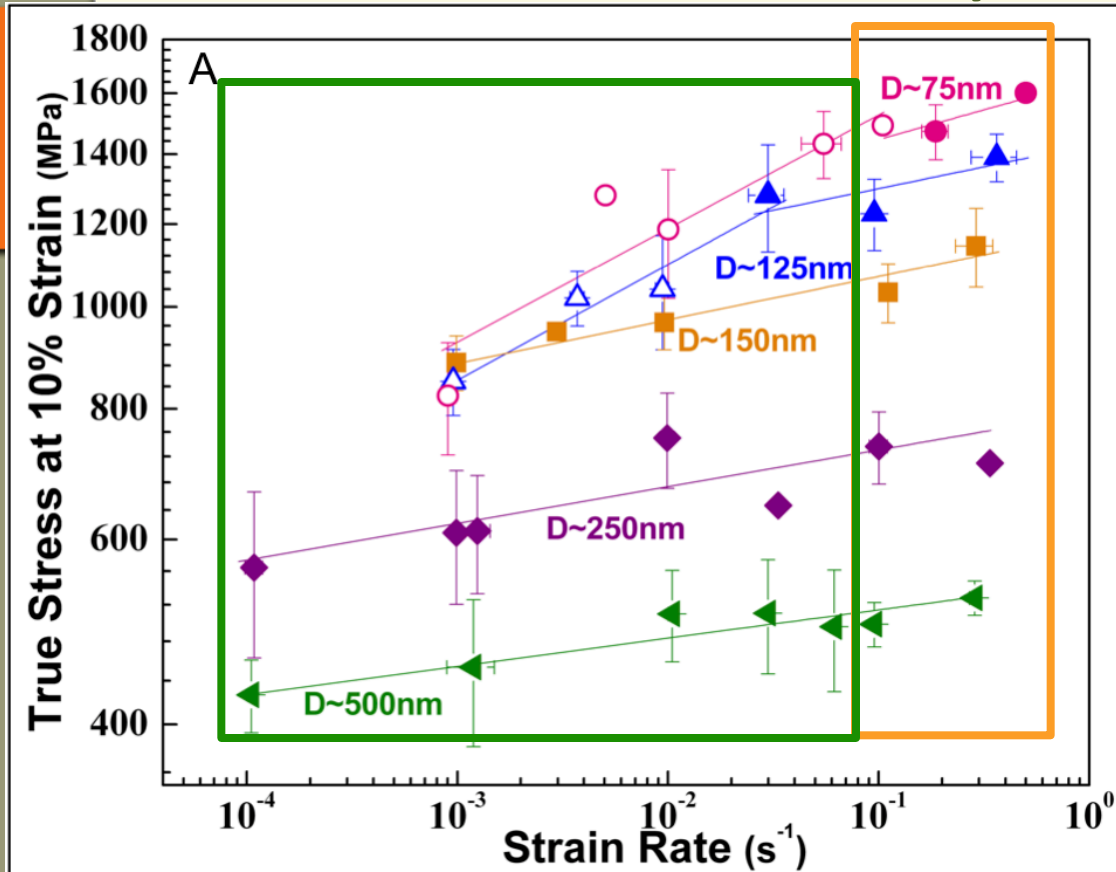


- Effect of Grain boundary: weakening by activation of GB-mediated processes
- - - Effect of Twin boundary: strengthening by impeding low-friction dislocation glide

Introducing **twin** boundaries increases strength
Introducing **grain** boundaries decreases strength



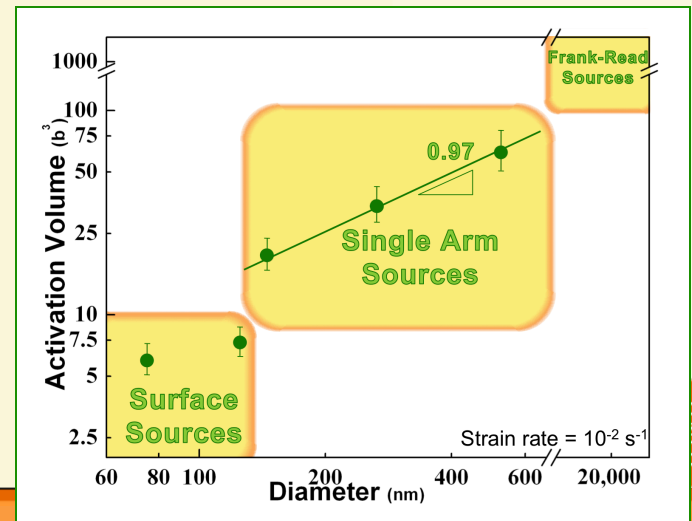
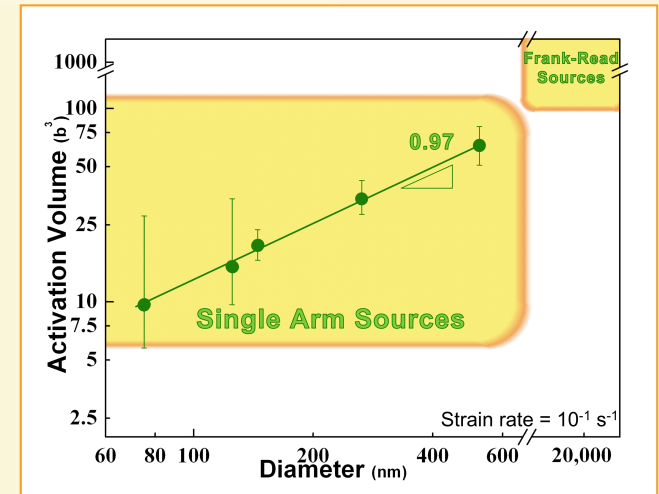
Strain Rate Sensitivity => Activation Volume



$$\sigma = \sigma_0 \dot{\epsilon}^m$$

$$\Omega = k_B T \frac{\partial \ln(\dot{\gamma})}{\partial \tau} \quad \tau = M\sigma$$

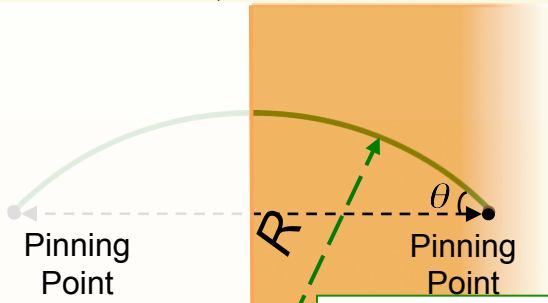
$$\dot{\gamma} = M\dot{\epsilon}$$



Transition to surface source operation may be manifested as deviation from the "athermal" size effect

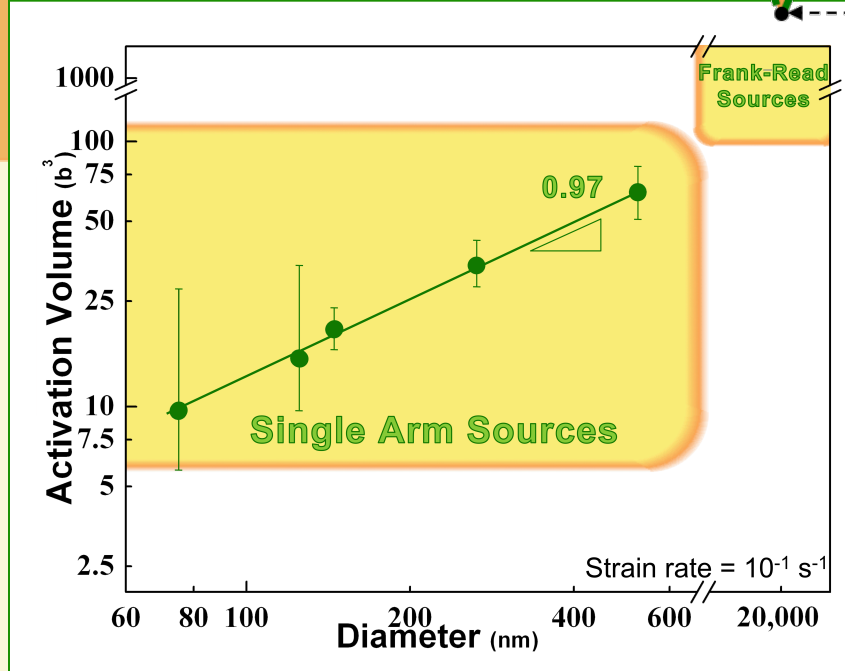
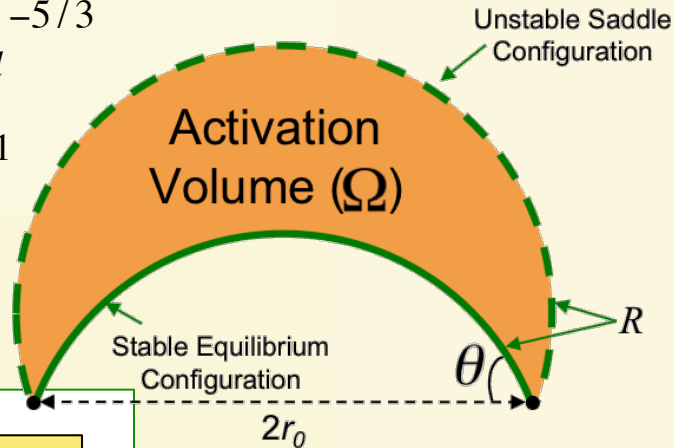
Activation Volume for a Single-Arm Source

1/2 of Frank-Read Source: $\Omega(\tau_{athermal}) \propto \tau_{athermal}^{-5/3}$
 $Q_{SAS} = 1/2 Q_{FRS}; \Omega_{SAS} = 1/2 \Omega_{FRS}$



$$\frac{\tau_{athermal} - \tau}{\tau_{athermal}} \ll 1$$

$$\tau_{athermal} \propto D^{-n}$$



$$= b(A^* - 2A_i) = br_0^2 f(\theta)$$

$$\tau_{athermal} = \frac{\mu b}{2r_0} \quad R \geq r_0$$

$$\frac{\tau_{athermal} - \tau}{\tau_{athermal}} \ll 1$$

$$\Omega \propto \frac{(\tau_{athermal} - \tau)^{3/2}}{\tau_{athermal}^{1/2}} \approx 0.7eV$$

$$f(\theta) \propto r_0^{-1/3}$$

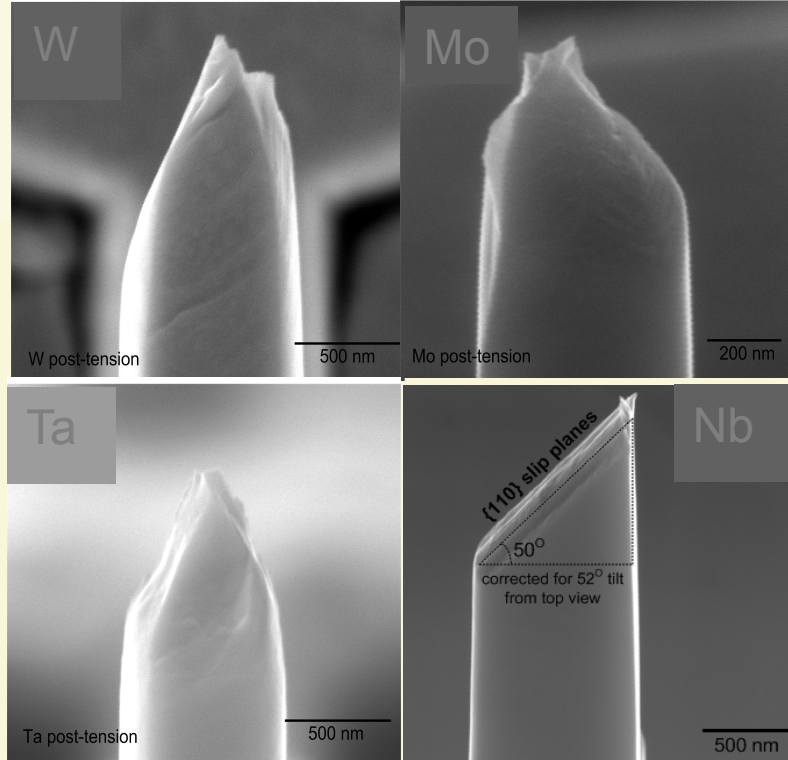
$$\Omega_{F-R} \propto r_0^{5/3}$$



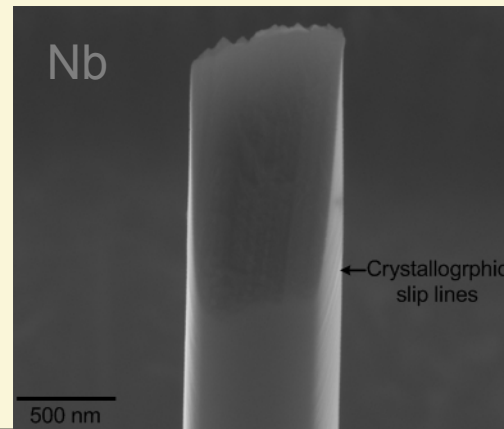
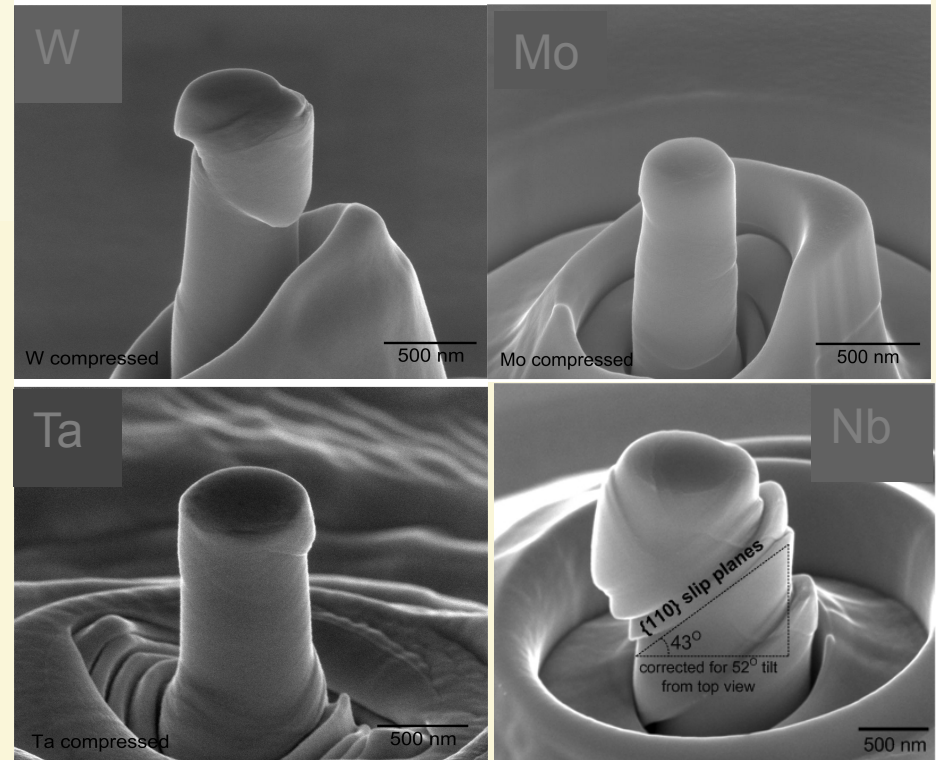
- Nabarro (1989)
- Shemenski (1965)
- Estrin et al (2007)
- Zhu et al (2010)

Moving onto BCC metals: Post-testing morphology

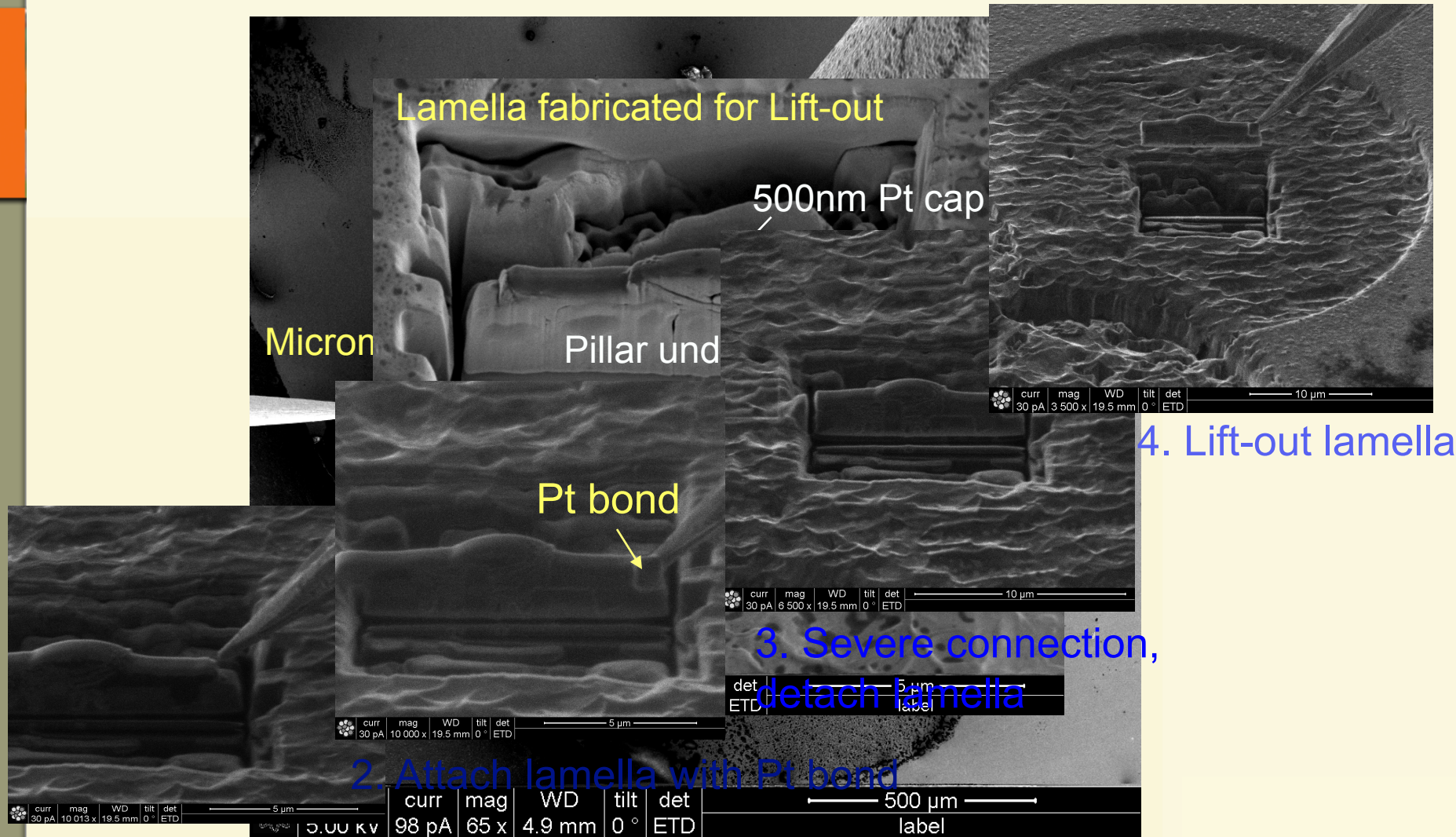
Pronounced shearing-off in tension



Crystallographic slip in compression



TEM Sample Preparation: Phase 1



TEM Sample Preparation: Phase 2

1. Bring in TEM grid

Pt Needle

Sample

TEM grid

Cross-section of lamella after some initial thinning

curr	mag	WD	tilt	det
30 pA	350 x	19.5 mm	1 °	ETD

HV	curr	mag	WD	tilt	det	2 μm
5.00 kV	98 pA	19 998 x	4.9 mm	54 °	ETD	label

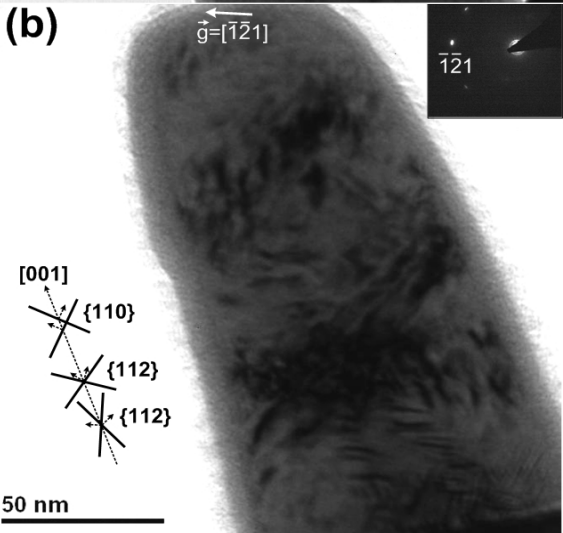
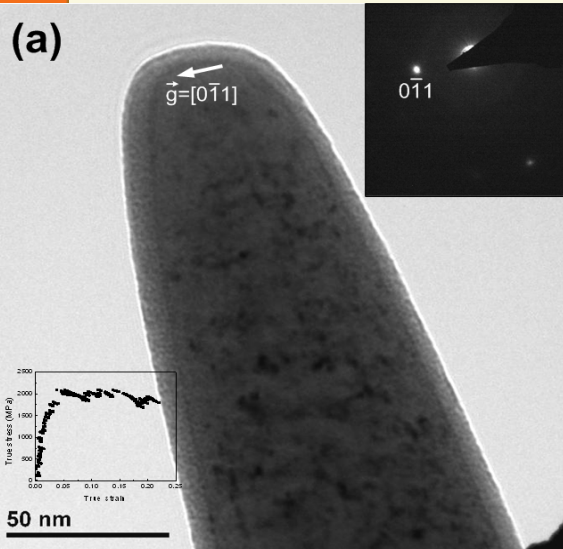
re the needle

curr	mag	WD	tilt	det	10 μm
30 pA	6 500 x	19.4 mm	1 °	ETD	

TEM Analysis of deformed pillars

Nb

Mo



⇒ Complex dislocation networks formed in Nb and Mo after compression

⇒ Partial dislocations generated on $\{110\}$, $\{112\}$, and $\{123\}$ planes in Nb

⇒ Dislocation segments are straight (rather than wavy) in Nb implying rare cross-slip

⇒ Dislocation density increases in Nb and Mo after compression

